THE EFFECTS OF ELEVATED TEMPERATURE ON THE BOND BETWEEN CONCRETE AND REINFORCING STEEL BARS.

By

R.J. CAWOOD, B.Sc., (ENG.) (CAPE TOWN).

A thesis submitted in partial fulfilment of the requirements for the Degree of Master of Science in the Faculty of Engineering, University of Cape Town.

Department of Civil Engineering.
UNIVERSITY OF CAPE TOWN.

April, 1974.

TABLE OF CONTENTS

Volume I.

SYNOPSIS

This investigation forms part of a larger programme undertaken to determine the mechanical, thermal, and time dependent property behaviour of concrete subjected to elevated temperature. A literature review covering the mechanics of bonding, viz. chemical adhesion, frictional effects and mechanical interaction is presented. Parameters which influence bond are discussed. These are properties of the steel reinforcing bar, properties of the concrete, embedment length, casting position of the reinforcing bar and temperature.

The research reported herein is primarily concerned with the effects of elevated temperature on the bond between concrete and steel. In this regard, a pullout bond test was used.

The parameters of the experimental programme included mix proportions, reinforcing bar diameter, type of rib pattern of reinforcing bar and temperature. Four mixes were used in this investigation. These had respective water/cement and aggregate/cement ratios of 0,44: 3,91; 0,44: 4,43; 0,60: 5,00 and 0,60: 6,21. The reinforcing bars had diameters of 12 mm and 25 mm respectively. For each of these diameters, two types of rib pattern were used, viz. plain and staggered, single helical patterns. Bond tests were performed at temperatures of 20°C, 70°C, 110°C, 160°C, 250°C and 350°C - specimens were heated for a total period of thirty two hours in specially designed heating jackets.

Test specimens were 305 mm x 250 mm diameter concrete cylinders, cast with the reinforcing bar in the vertical position along the longitudinal axis of the cylinder. The conventional test method for measuring bond strength

was modified by the use of an annular bearing surface situated at the circumference of the test specimen and by preventing bond between the concrete and steel for 100 mm from the bearing concrete surface. These modifications are shown to develop a zone of tensile longitudinal concrete stress next to the concrete steel interface, and to produce loaded end slip results which are more indicative of slip in actual reinforced concrete members than those obtained from the conventional test.

The investigation determined the effects of temperature on bond strength, slip at unloaded end and slip at the loaded end. The contributions of bar diameter and mix proportions towards the deterioration of slip resistance with increase in temperature was also determined.

The results established that the bond strength of ribbed bars shows similar patterns of deterioration with increase in temperature as the compressive and tensile strength of concrete. In this respect, deterioration of bond strength was greatest at 110^{o}C with recovery at higher temperatures. Plain bars did not exhibit any recovery of bond strength. Loss of bond strength at all temperatures was greater in the case of plain bars than for bars with ribs.

With reference to the unloaded end slip, it was found that slip resistance decreased with increase in temperature. As in the case of bond strength, greatest reduction of slip resistance was manifest at 110^{o}C for ribbed bars. Slight recovery of slip resistance occurred at higher temperatures. Plain bars showed no recovery of slip resistance because of the large influence of temperature on adhesion bond. Although bar diameter was found to influence the average bond stress at a particular slip, this parameter had no effect on the deterioration of the bond with increase in temperature. Mix proportions affected the average bond stress of plain and ribbed bar specimens at temperatures below 110^{o}C.

The investigation of loaded end slip indicated similar trends for the deterioration of bond as determined from the unloaded end slip. However, it was observed that less loaded end slip occurs at 70°C than at 20°C for all types of bar. This was attributed to the greater deformation and cracking of concrete near the loaded end at the higher temperature.

An axisymmetric finite element analysis of the bond specimen was performed to determine the distribution of stress in the concrete matrix. The analysis assumed perfect bond between concrete and steel. Results indicated that the modified test method produces tensile longitudinal stresses along the bonded length of interface. The analysis also showed the importance of concrete deformation on the measurement of slip at the loaded end. Loaded end slip in the conventional test was found to be 30% greater than that in the modified test.

A second analysis assumed slip between the concrete and steel of a plain reinforcing bar. In this respect, a linkage element was used to simulate slip. The analysis estalbished that stresses were considerably reduced by slip.

ACKNOWLEDGEMENTS.

The Author is indebted to his thesis advisor Professor W.H. King for his guidance during this investigation, especially for his criticism and suggestions during the writing of this thesis.

Thanks are due to the staff of the Department of Civil Engineering for their help and co-operation - particularly the laboratory and workshop staff for their assistance in the practical work of this investigation.

Thanks are also due to Mr. F.J.P. Roux for his encouragement and guidance during the author's graduate study.

The author would like to acknowledge the financial support provided for this work by the Electricity Supply Commission and the University of Cape Town.

CHAPTER 1 - INTRODUCTION.

1.1) Nomenclature

Bond: The resistance of concrete to any force that tends to pull or push out a reinforcing bar embedded in the concrete.
Bond Stress: Unit shearing force acting parallel to the bar on the interface between bar and concrete.
Bond Strength: Ultimate bond stress value at failure load.
Deformed Reinforcing Bar: Reinforcing bar whose bond is increased by transverse and longitudinal ribs.
Plain Reinforcing Bar: Mild steel as rolled bar without ribs for increasing bond.
Loaded End: End of bond specimen at which load is applied to the reinforcing bar.

1.2) Bond

The function of bond in a reinforced concrete member is to hold the two materials together (concrete and steel) so as to develop their simultaneous and mutually helpful action. The two materials do not have similar elastic properties and application of load to a composite member causes one of the components to strain relative to the other. Consequently, a shear stress occurs at the concrete steel interface i.e. bond is developed. When the shearing force becomes sufficiently large to overcome the resistance offered by the bond, bond failure results.

The interaction between the steel and concrete in a member subjected to tensile stress consists of two processes. Firstly, the tensile force is transferred from the concrete to the steel and bond stresses are developed so that the steel takes its appropriate share of the tension. Secondly, the strain thus induced in the steel becomes greater than the strain in the adjacent concrete

and must be retransmitted to the concrete at this point, so that a stress is induced in the concrete opposing the stress at the original section of transfer. Nodes of maximum tensile stress and strain are set up in the concrete and at each node cracks can be expected to form. The distance between cracks is influenced by the bond between the concrete and steel. The bond developed is thus of major importance in ensuring the integrity of a particular design.

Bond stress in a beam may be defined either as the nominal 'flexural' or 'local' bond value, calculated from the expression:

$$\text{Local bond stress } U = \frac{Q}{L \times O} \qquad \ldots\ldots(1)$$

where Q = total shear across the section
L = arm of the resistance moment
O = sum of the perimeters of the bars in the tensile reinforcement,

or it may be defined as the average bond stress from the point of maximum tension to the end of the bar by the equation

$$\text{Average bond stress } T = \frac{P}{\Sigma(p \times L)} \qquad \ldots\ldots(2)$$

where P = change in load along length of the bar considered
p = perimeter of bar
L = length of bar

The latter bond stress term has been called 'anchorage' or 'development' bond and it is believed to be more meaningful than the 'flexural' or 'local' bond value.

1.3) Testing for Bond.

Bond strength is determined by either beam tests or pullout tests. The pullout tests are satisfactory for measuring the relative bond values of bars with different

deformations. Bond values derived from pullout tests cannot be applied in general to the design of reinforced concrete structures - beam tests are necessary to develop design criteria.

1.4) Bond Strength Tests.

Bond strength tests must simulate as closely as possible the actual manner of loading in a structure. Bond failure may occur under three types of loading, acting either alone or in combination.

a) Concrete and steel in tension. (beams)
b) Concrete and steel in compression. (columns and beams)
c) Concrete and steel in shear. (stirrups)

There are three basic methods of testing the relative bond efficiency of different reinforcing bars. These are:

i) Pullout (or pushout) tests.
ii) Beam tests.
iii) Torsion tests.

No single bond test simulates all the loading conditions indicated above.

i) Pullout Tests.

The pullout test is the most commonly used method of testing bond strength. A typical pullout specimen and test rig is illustrated in Figure 1. A bar is cast horizontally or vertically in a block, cube or cylinder of concrete. The bar is pulled from the concrete and the relative slip between steel and concrete at either or both ends is measured by means of a dial gauge clamped to the bar or the concrete specimen. This test method

has the advantage of being cheap and easy to perform for comparing the bond strengths obtained with different mixes, water-cement ratios and methods of compaction. However, an objection has been raised against the pull-out test. This is due to the fact that the bond slip curves derived from conventional pullout tests are not indicative of those produced in actual structural members, i.e. the concrete is in compression and steel in tension during the pullout test whereas the concrete surrounding the tensile reinforcement in a structural member is usually in tension. Thus, in the pullout specimen the slip is the total steel elongation in the specimen length plus any compressive shortening which may exist in the concrete. In a beam, the slip is the steel elongation minus the elongation of the concrete in tension. Furthermore, the pullout test does not represent the horizontal shearing stresses which exist in considerable magnitude at the level of the bars in a beam.

The above shortcomings of the conventional pullout test are eliminated in the lapped or butted bar pullout test. In this test the load is applied to the bars and the concrete is placed in tension. The butted bar test simulates a portion of a beam between two cracks.

Pushout tests are a development of pullout tests. Both the concrete and steel are placed in compression. Results differ from those obtained in pullout tests because of the dilatance of the bar under load increasing the pressure between the concrete and steel.

ii) Beam Tests.

These tests of actual beams usually consist of applying a bending moment by single or preferably two or four point loading until failure occurs. This test simulates more closely the conditions under which reinforcing bars

operate i.e. the steel and concrete are both in tension simultaneously. A typical beam specimen is illustrated in Figure 2. The beam test specimen is modified to remove the pressure under the bar provided by the reaction restraint. (Untrauer and Henry [24] have shown that lateral pressure on a specimen containing a bar does increase bond resistance substantially).

In general, there is little correlation between the bond stress versus slip curves obtained from pullout and beam tests. [21] Beam specimens are weaker in bond because of the ill effects of flexural cracking but loaded end slip is smaller in the case of beams because the flexural cracks tend to distribute the elongation of the steel in several places.

iii) Torsion Tests.

These tests have been used to a very limited extent to obtain bond strengths. [1] [25] They consist of twisting the bar about its axis relative to the concrete. The rotation of the bar relative to the concrete is obtained at both loaded and free ends by means of suitable levers and dial gauges. This test does not appear to have any parallel under normal loading conditions.

1.5) Objectives.

The objectives of this investigation were to:

(a) Determine the effect of elevated temperatures on the bond between concrete and steel,

(b) Develop a modified pullout test to simulate experimentally the deformation of the concrete produced in a structural member and to compare the results with those produced from conventional pullout tests,

(c) Develop an axisymmetric finite element programme

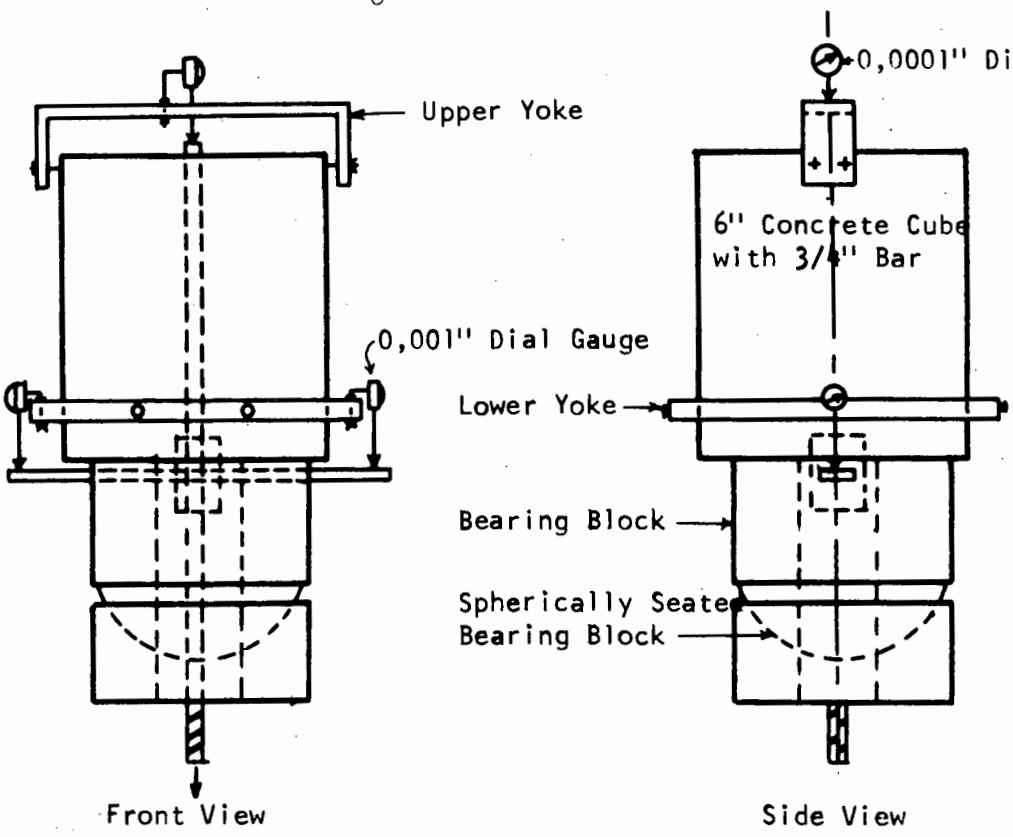

FIGURE 1 ASTM (234-62) BOND TEST

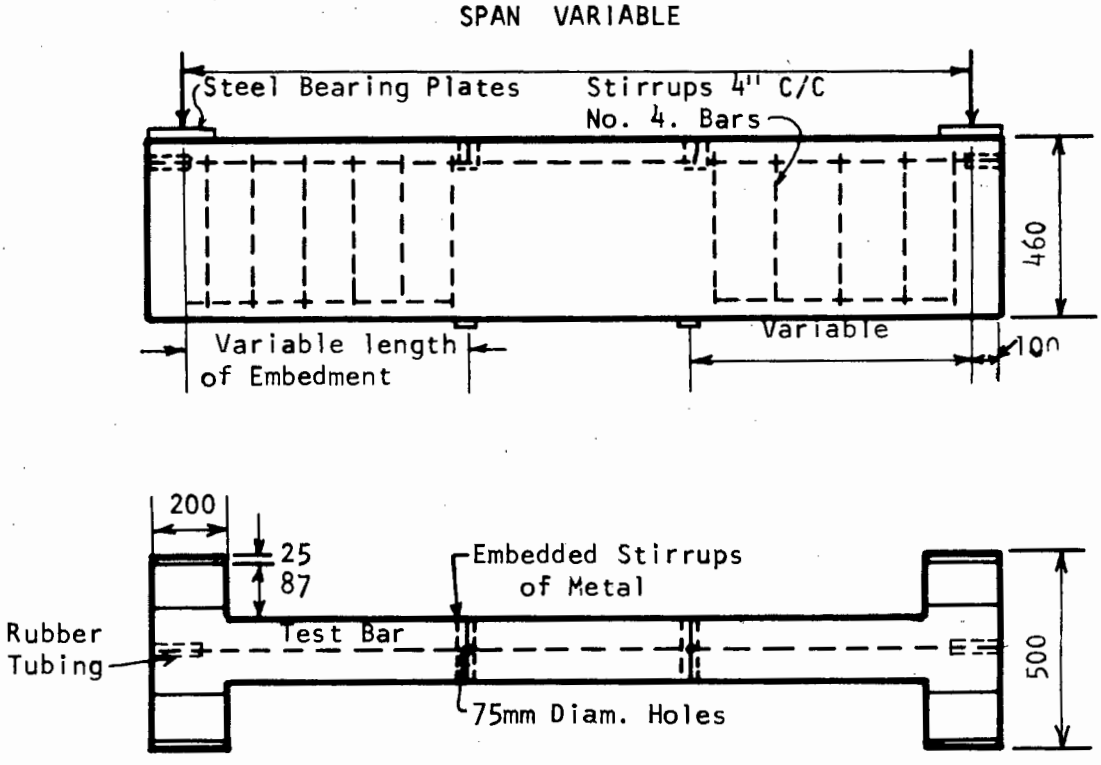

All Dimensions In mm Unless Otherwise Indicated

Figure 2 Test Beam To Permit The Measurement Of Average Value Of Bond Stress At Free And Loaded Ends [21].

to analyse the stress conditions set up by the modified pullout test and compare it with the stress distribution obtained from conventional pullout tests.

(a) The Effect of Elevated Temperatures on Bond.

Reinforced concrete is a material suitable for constructing the containment structure of a Nuclear Reactor. This is primarily because concrete provides good shielding of electromagnetic radiation and nuclear particles at a relatively low cost. However, the mechanical properties of concrete are adversely affected by the elevated temperatures encountered in the containment structure of a Nuclear Reactor. In this regard, very little research has been done on the effect of temperature on bond, despite the indications that bond strength is one of the mechanical properties most susceptible to deterioration when concrete is heated.

(b) Modified Pullout Test.

A modified pullout test has been used in the experimental investigation of this thesis. For reasons mentioned earlier the conventional pullout test is unreliable for producing design criteria and has thus been modified to produce tensile longitudinal stresses along the length of the concrete - steel interface and to allow deformation of the concrete at the loaded end.

The cylindrical pullout specimen which has a diameter of 250 mm uses an annular bearing surface as indicated in Figure 3. The bearing surface is 50 mm wide and is situated at the circumference of the loaded end concrete surface. An unbonded length of 100 mm from the loaded end is also introduced. Reasons for this will be given in Chapter 3. The application of a load to the bar produces loaded end concrete deformation and a zone of longitudinal tensile

stresses which stretches back to the end of the specimens as indicated in Figure 3.

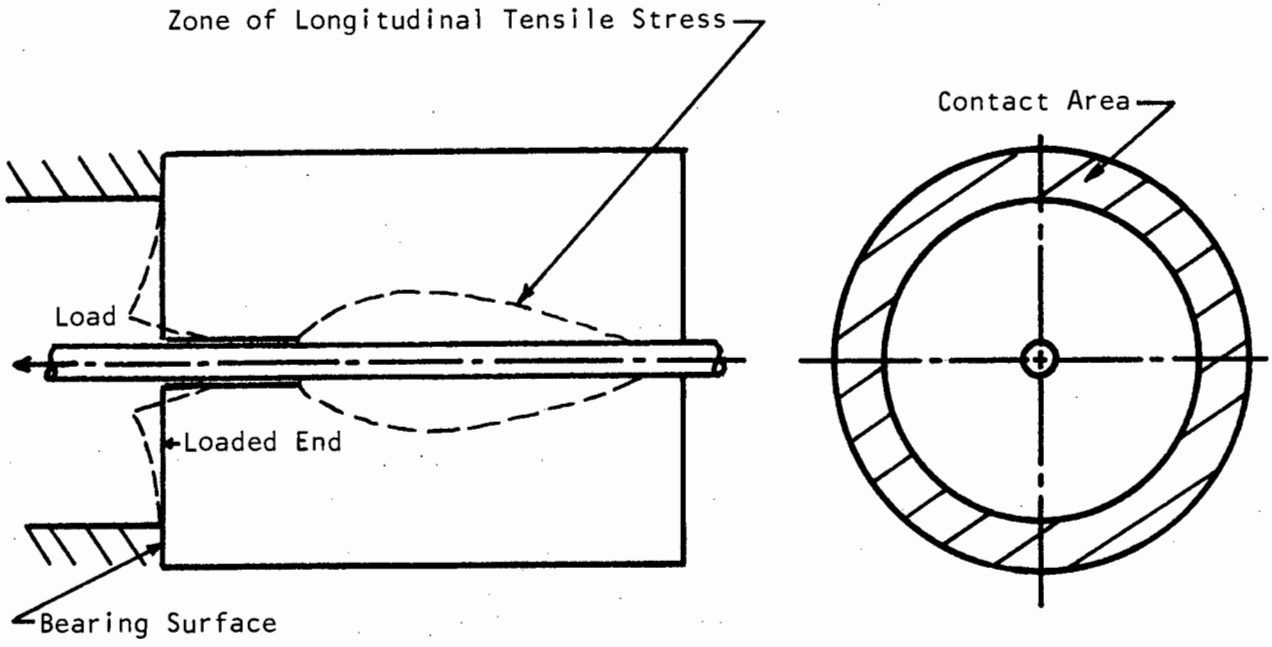

Figure 3 Modified Pullout Test Bond Specimen

The modified bond strength test results are compared with those of the conventional test method. It should be noted that the conventional test specimens tested in this investigation do not comply with ASTM or SABS standards. A larger specimen is used in the present tests - (diameter 250 mm and length 205 mm). However, the test method is the same as that used in the standards. It is difficult to draw direct comparisons with results published by other investigators. This is because of the numerous different test methods employed and the number of parameters which affect bond. Furthermore, relevant information such as concrete strength and workability, rust condition of bars and geometry of ribs is often omitted from reports on bond strength. Consideration must

also be given to the fact that the bond test produces a wide scatter of results and their interpretation may differ from one investigator to another.

(c) Axisymmetric Finite Element Analysis of Stress.

A finite element analysis of the stress distribution in the bond specimen has been developed. This was necessary to verify the assumption of tensile stresses at the interface as mentioned above. In the process of the programme, an attempt has been made to simulate the initial slip conditions under load and to determine its effect on the stress distribution. A comparison between the stresses and displacements of the concrete produced by low loads in the conventional pullout test and those produced in the modified pullout is made.

CHAPTER 2 - THE REVIEW OF LITERATURE.

2.1) The Mechanics Of Bond And Slip.

In reinforced concrete the bond between reinforcing steel and concrete is due to:

(i) Chemical adhesion
(ii) Friction
(iii) Mechanical interaction between the concrete and irregularities on the reinforcing bar.

These effects may act independently or in combination, depending upon the type of bar used and the intensity of the bond stress.

There are principally two types of bar; plain bars and deformed bars. Each will be considered separately.

(i) Plain Bars.

Plain reinforcing bars develop their bond primarily by chemical adhesion and friction. Adhesion is usually considered to take the entire bond force before slip occurs while friction takes the load after slipping has begun. However, the roughness of the bar, i.e. mechanical interlocking on a small scale, influences both the measured adhesion and friction.

The strength of adhesion is not accurately known. It has been shown to be small and quite variable. Values of between 0,543 N/mm^2 and 1,708 N/mm^3 have been quoted. (29) Adhesion is likely to be significant only in regions where compressive force and shear are applied to the bar, but rather insignificant in regions where tension exists at the bar concrete interface.

Good frictional properties are essential for good bond with plain bars. For frictional forces to become effective, a normal pressure is required at the concrete steel interface. This normal compressive force is due to shrinkage and a pinching effect which occurs near a transverse crack as illustrated in Figure 4.

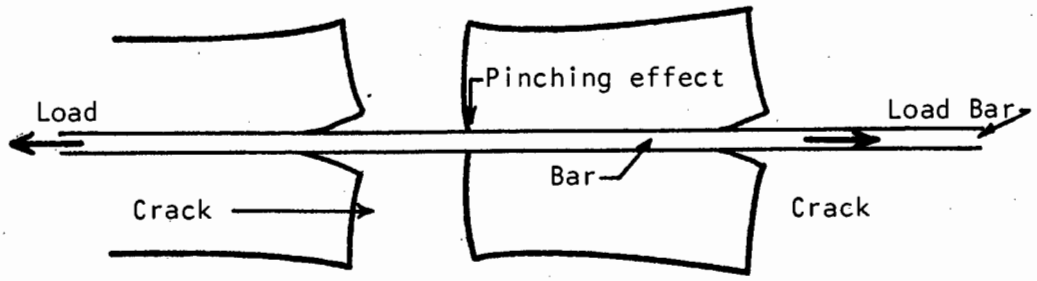

Figure 4 Transverse Crack.

Frictional resistance also develops from surface roughness due to mechanical interlocking. At high stresses the Poisson's ratio of the steel, spreading tendency of the concrete at a transverse crack, plus splitting will cause the concrete and steel to separate and lose all frictional contact.

In pullout tests, the mechanism of bond fracture between plain reinforcing bars and concrete is due to a crack propagation in the concrete close to the interface. This crack develops from the external face where the bar protrudes from the concrete mass and propagates inwards as the load increases above that at which cracking commences. Within the concrete mass, failure is due to shearing between the steel and the concrete matrix. (vide Appendix 1.1).

Brown [3] has developed an equation for the load transfer from steel to concrete in the frictional stage. His theoretical hypothesis is based on the tribophysics of

the steel concrete interface and Goodiers extension of St. Venants Principle. (vide Appendix 1.2). The mode of transfer of the load from the steel to the concrete due to a monotonic loading sequence is indicated in Figure 5a, 5b, 5c. A load increment ΔF applied to the composite body is resisted by the rod, δF, and the concrete, $\Delta F - \delta F$. As the load increases the average shear stress capacity of the concrete, Tc, is exceeded and a crack propogates a distance Δl along the rod. The load transfer of $\sum_{i=1}^{n} (\Delta Fi - \delta Fi)$ from the steel to the concrete is thus:

$$F - Fs = \sum_{i=1}^{n} (\Delta Fi - \delta Fi) = 2\Pi (rb + dc) \int_0^{\ell} T_c(x)\, dx \quad \ldots\ldots 1$$

Where rb = diameter of the reinforcing bar

dc = average distance of the crack from the steel bar.

Tc(x) = average shear stress capacity of concrete at a distance x from the loaded end.

Peattie and Pope [1] have shown that the distribution of load in the steel during the chemical adhesion stage of bond stress, i.e. $x>\ell$, is;

$$F_1 = Fm \cdot e^{-kp} \quad \ldots\ldots 2$$

Where F_1 is the load on the bar at a distance p from the rupture point.*

*The rupture point is defined as that point at which load is no longer developed by chemical adhesion only, i.e. due to relative movement between the steel and concrete, a frictional effect becomes partly responsible for slip resistance.

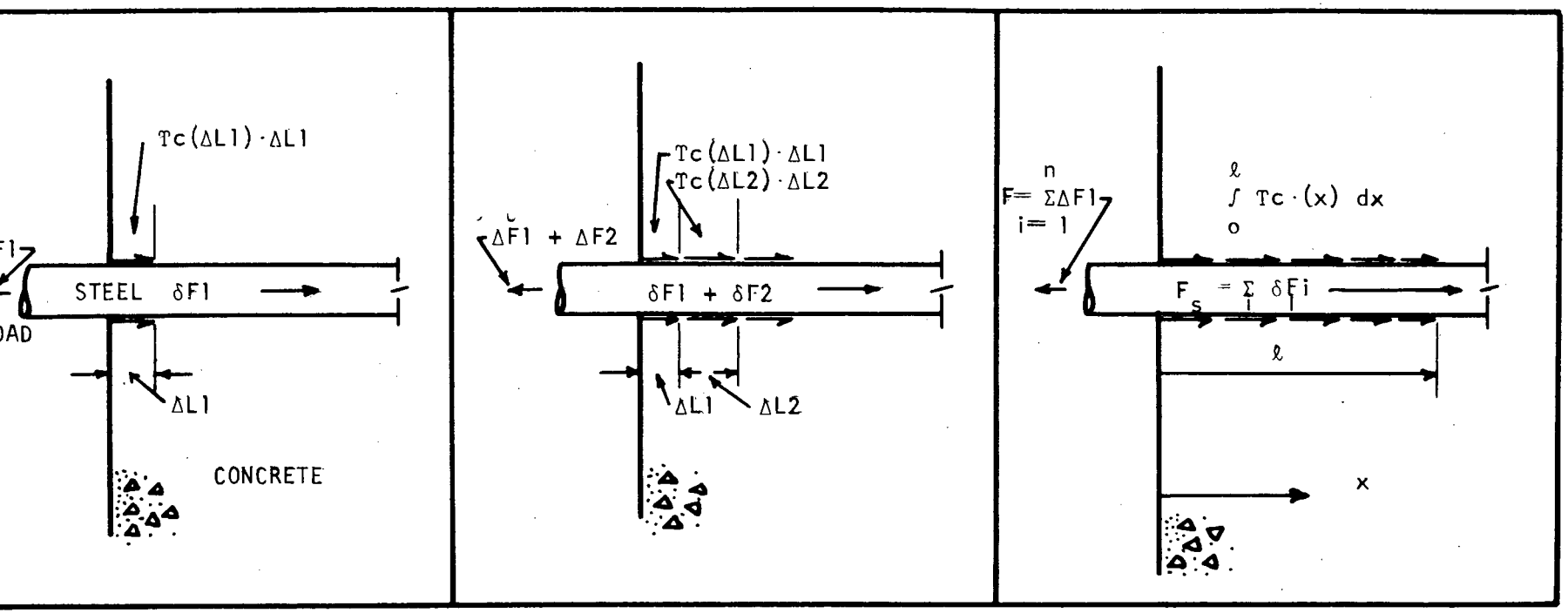

FIGURE 5a

FIGURE 5b

FIGURE 5c

FIGURE 5 EFFECTS OF MONOTONIC LOADING SEQUENCE (3)

Fm = the load at the rupture point necessary to produce rupture at that point.
k = exponential coefficient
p = the length of embedment from the rupture point.

The distribution of load in the frictional stage is assumed to be given by:

$$Fa = \ell . rb (b + c.\ell)$$

where b,c = frictional coefficients
rb = the reinforcing bar diameter
ℓ = the distance from the loaded end to the rupture point.
Fa = the load in the bar additonal to Fm.

The distribution of load in both stages is shown in Figure 6. It is apparent from Figure 6 that as the applied load increases, the rupture point moves further away from the loaded end.

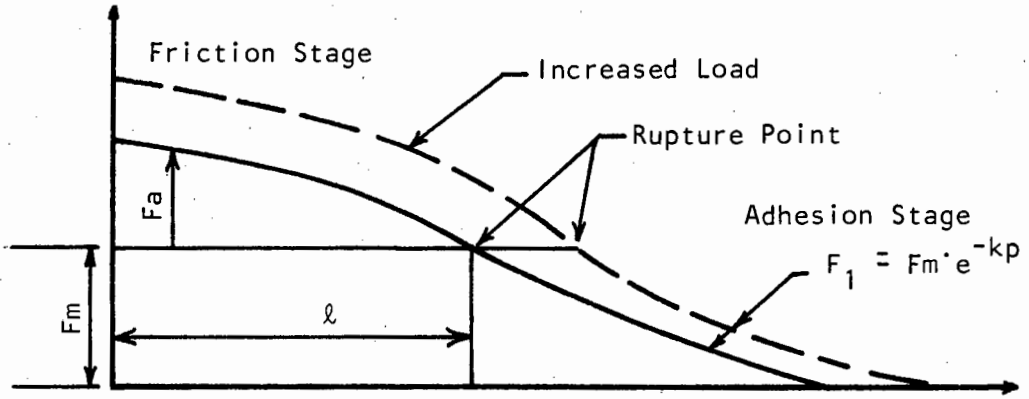

Figure 6 Load Distribution In Plain Reinforcing Bar[1]

(ii) Deformed Bars.

The mechanics of bond and slip of deformed reinforcing bars is similar to that of plain bars but only during the initial stages of load application. Initially chemical adhesion combined with mechanical interaction prevent slip. After adhesion is destroyed and slip occurs, the ribs of the bar restrain this movement by bearing against the concrete between the ribs.

Deformed reinforcing bars slip by either:

(a) wedging action of the ribs pushing the concrete away from the bar, or
(b) crushing of the concrete in the vicinity of the ribs.

For small values of the rib face angle (shown as θ in Figure 7) wedging action governs the magnitude of slip after the initial chemical adhesion and frictional effects have been overcome. For rib face angles greater than 45°, the friction between the rib face and the concrete is sufficient to prevent relative movement between the steel and concrete interface. Consequently, the relative movement between the bar and the concrete is entirely due to crushing of the concrete in the vicinity of the rib. In this respect tests by Lutz [2] have shown that although greater slips are produced by greasing the ribs, at high loads and for large rib face angles, surface conditions of the rib do not effect slip. However, for slip resistance at low stresses and, or low values of θ, the frictional properties of the rib face should be good.

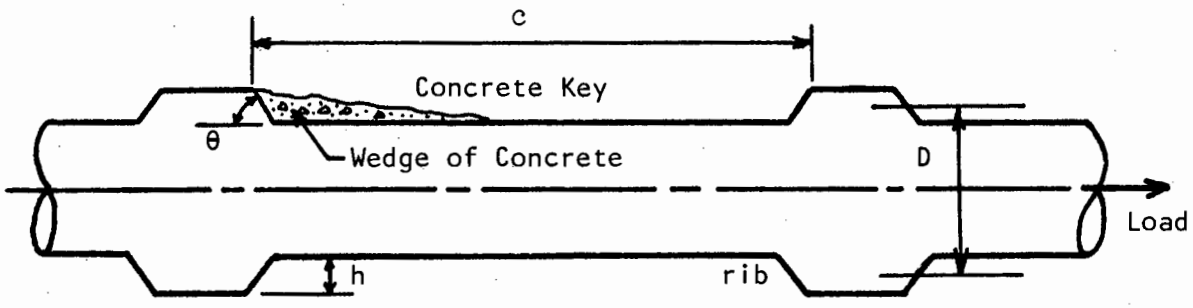

c = Rib spacing
h = Rib height
θ = Rib face angle
D = Nominal diameter of bar

Figure 7 Geometry Of Deformed Reinforcing Bar.

Bernander [15] determined the steel stress distribution along ribbed bars experimentally and found it to be parabolic. This indicates a linear distribution of bond stress. Thus the equation for bond stress distribution may be assumed to be:

$$r = r_o \frac{L - x}{L}$$

where r_o = bond stress at the loaded end
L = length of embedment
x = distance from the loaded end.

Effective anchorage lengths were calculated using this equation and found to compare favourably with measured results. (vide Appendix 1.3). This law of bond stress distribution only applies to cases where the whole embedment length is not yet used, i.e. at comparatively low steel stress (1000 kg/cm^2).

Rehm [4], [5] derived a differential equation for slip by considering a non-linear load slip relationship determined from his tests. He states that the rate of change of slip with distance is equal to the difference between the strain in the steel and the strain in the concrete at any point along the length of bar. A constant concrete stress is assumed to exist over the concrete section and can thus be related to the steel stress. In this manner the bond stress is simplified to the rate of change of the steel stress with distance.

The compression under the shoulder of the rib is related to the cube compressive strength by the equation:

$$X_R = \frac{T}{w_b}$$

where T = compressive stress on shoulder of rib
w_b = cube compressive strength.

X_R is called the 'relative compression' value.
The relative compression is related to the slip as indicated in Figure 8 and from these curves the following relationship is postulated:

$$X_R = C \cdot \Delta^{\alpha} \qquad 0 \leq \alpha \leq 1 \qquad \ldots\ldots 5$$

where Δ = local length of slip
C = constant

Rehm assumes that equation (5) is valid at any point on the length of the bar. With these relationships a second order differential equation is developed in terms of slip.

$$\frac{d^2 \Delta}{dx^2} = k^2 . \Delta^{\alpha} \qquad \ldots\ldots 6$$

where $$k^2 = \frac{1 + n\mu}{E} \cdot \frac{4}{d} \cdot Wb \cdot Fr \cdot C \qquad \ldots\ldots 7$$

$$n = \frac{E}{E_c}$$

E = Youngs modulus of steel
E_c = Youngs modulus of concrete
d = diameter of bar
Wb = compressive strength of concrete
Fr = surface of support of the rib
C = constant

$$\mu = \frac{Ac}{As}$$

Ac = Area of concrete
As = Area of steel

Equation (6) was used to determine the steel stress versus embedment length and bond stress versus embedment length curves illustrated in Figure (9) and (10). (vide Appendix 1.4) These figures illustrate that the slip resistance, T, increases as the slope of the curves of relative compression versus length of slip become greater. The plain bar steel stress distribution, $\alpha = 0$, is thus linear and a constant value of the bond stress distribution is obtained.

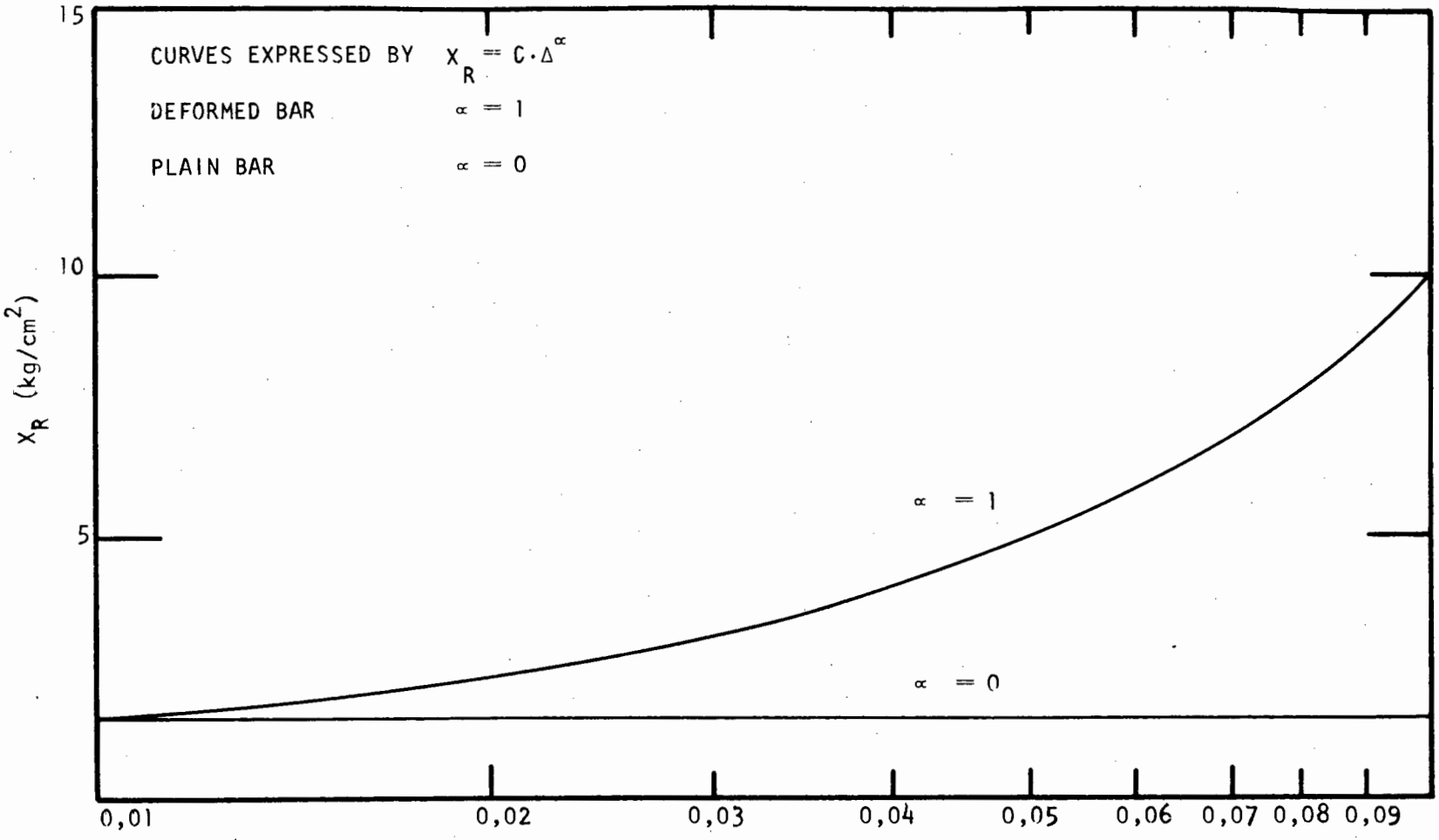

Figure 8 Relative Compression Versus Length Of Slip (4)

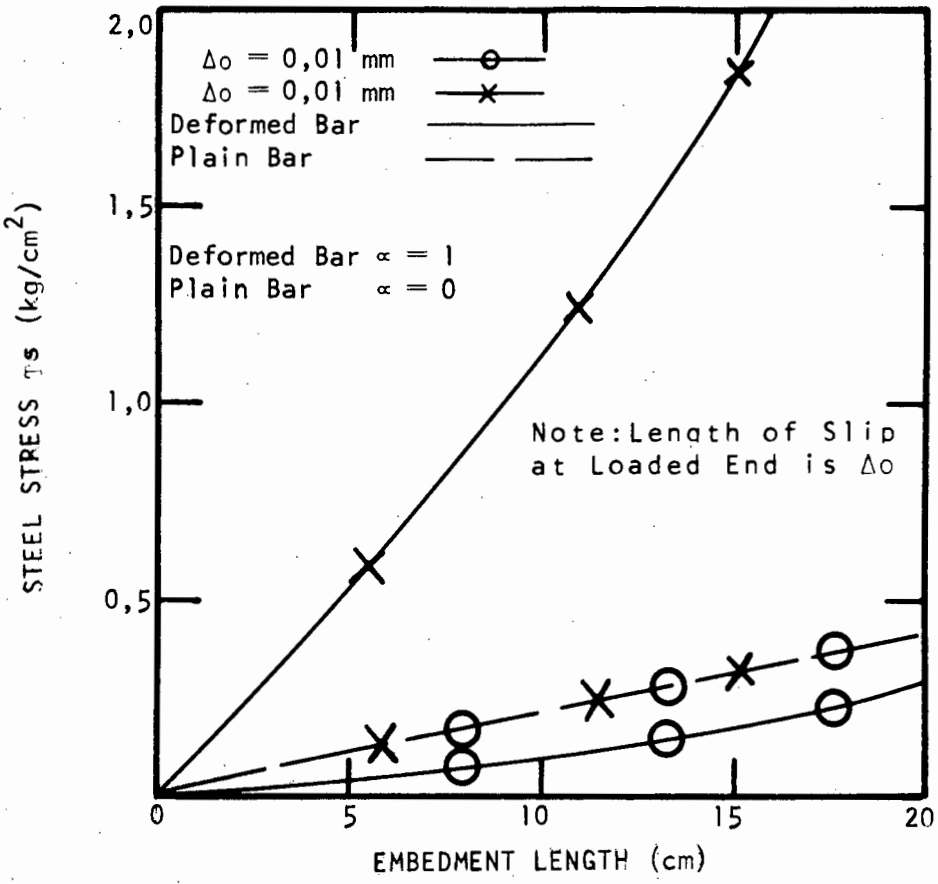

Figure 9:Steel Stress Versus Embedment Length (4)

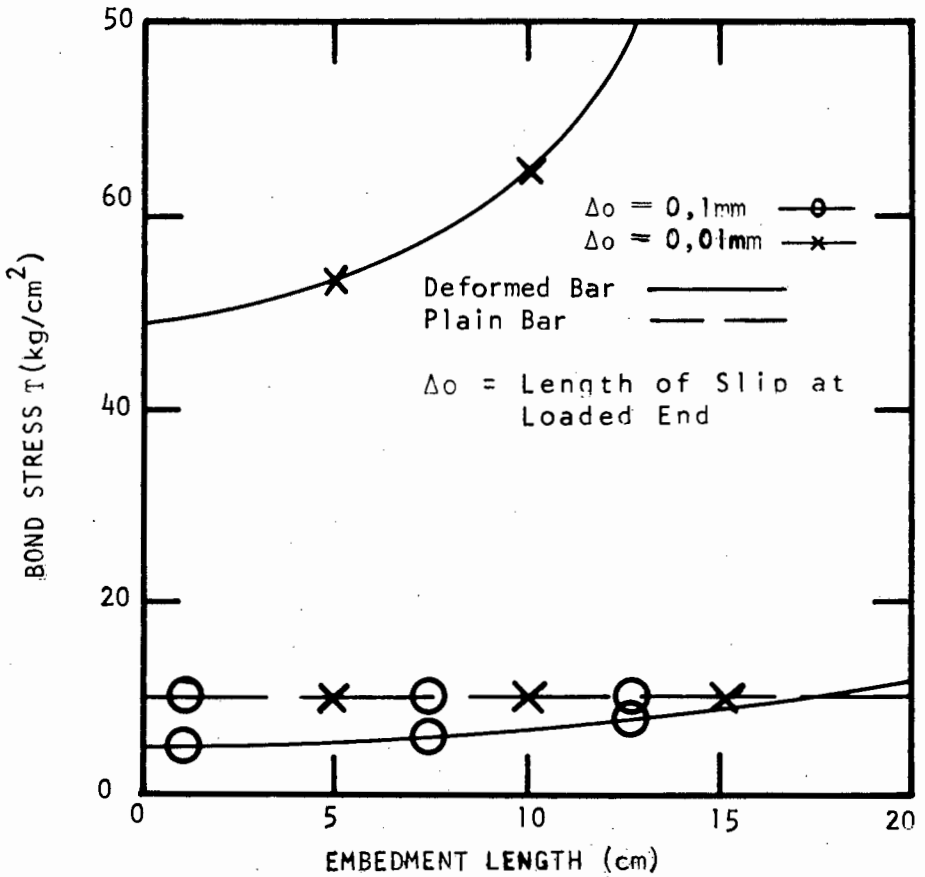

Figure 10:Bond Stress versus Embedment Length (4)

Summary

The bond between concrete and reinforcing steel has been shown to be due to chemical adhesion, friction and mechanical interaction.

Chemical adhesion and friction are primarily responsible for the bond of plain bars. However, mechanical interaction of the irregularities of the bar with the concrete influences the slip resistance. Bond due to adhesion is small and a wide range of values for the adhesion bond stresses have been determined. Frictional bond resistance is developed by the shrinkage of the concrete after casting and is improved by the pinching effect of the concrete at transverse cracks.

The mechanism of bond of plain bars is a crack propagation along the bar as the load is increased. Two distinct stages of bond are thus realized, the frictional and adhesion stages. The stress distribution in the frictional stage is a function of the bar load and distance from the rupture point to the free end - that in the adhesion section is dependent on the bar diameter and the distance from the loaded end to the rupture point.

Deformed bars develop their bond primarily by mechanical interaction of the concrete and ribs. The influence of adhesion is negligible. Slip can occur through the wedging action of the ribs or crushing of the concrete. The mechanism of slip is influenced by the rib face angle and it has been shown that for values of θ greater than 45°, the slip is entirely due to crushing of the concrete at the interface.

The steel stress distribution along deformed bars has been experimentally shown to be parabolic. Equations for determining the bond stress distribution have been postulated.

2.2) Factors Affecting Bond Resistance.

The factors primarily affecting bond resistance are:

(i) Properties Of Reinforcing Steel Bar.

- (a) Deformation Pattern
- (b) Bar Diameter
- (c) Height of the Rib
- (d) Rib Spacing
- (e) Rib Face Angle
- (f) Rust and Scale

(ii) Properties Of The Concrete.

- (a) Compressive Strength
- (b) Tensile Strength
- (c) Maturity of the Concrete
- (d) Workability of the Concrete

(iii) Embedment Length.

(iv) Casting Position Of Reinforcing Bar.

(v) Temperature.

(i) Properties Of The Reinforcing Steel Bar.

Properties of the bar which will be considered are:

(i) Geometrical properties viz. shape of the deformation pattern, bar diameter, rib height, rib spacing and rib face angle.

(ii) Properties of the surface condition viz. rust and scale.

(a) Deformation Pattern.

Various authors[5] [7] have found that the bond developed between concrete and reinforcing bars is dependent upon

the geometry of the rib and to a lesser extent the deformation pattern of the steel. The most common types of deformation pattern are illustrated in Figure 11. Of these, bars with helical patterns appear to produce the best results. This is substantiated by the steel stress versus slip curves for different types of deformation pattern, illustrated in Figure 12. From this diagram it is apparent that steel stresses can be more than twice as high in helical bars than in plain reinforcing bars at the same loaded end slip.

(b) Bar Diameter.

In a given embedment length a small bar causes higher stresses in the vicinity of the bar than a larger bar at the same load due to the smaller bar perimeter. However, the stress condition away from the bar is quite similar due to the equal bar loads.

Lutz [2] has indicated that in plain bars where friction on the bar perimeter governs the bond strength, the bar load tends to be a function of the bar diameter. This is because the bond strength of plain bars is greatly influenced by the distress of the concrete in the vicinity of the bar.

Ferguson [8] et al compared the efficiencies of three different diameter deformed bars, viz, 22,0 mm, 43,0 mm and 57,5 mm. In Figure 13 a comparison of bond stress is made using the ratio of loaded end slips to the bar diameter. The curves of bond stress versus slip are seen to converge. These curves indicate that for a particular bond stress:

(a) loaded end slip varies approximately in proportion to the diameter,
(b) greater slips are produced by the larger diameter bars.

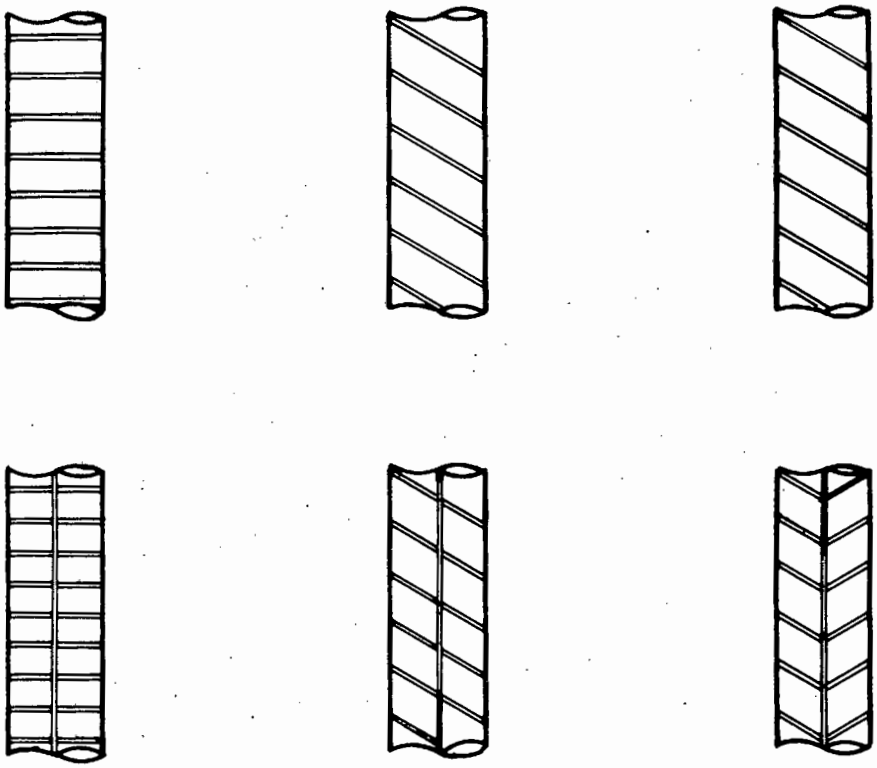

TRANSVERSE

DOUBLE HELICAL CONTINUOUS

DOUBLE HELICAL REVERSED.

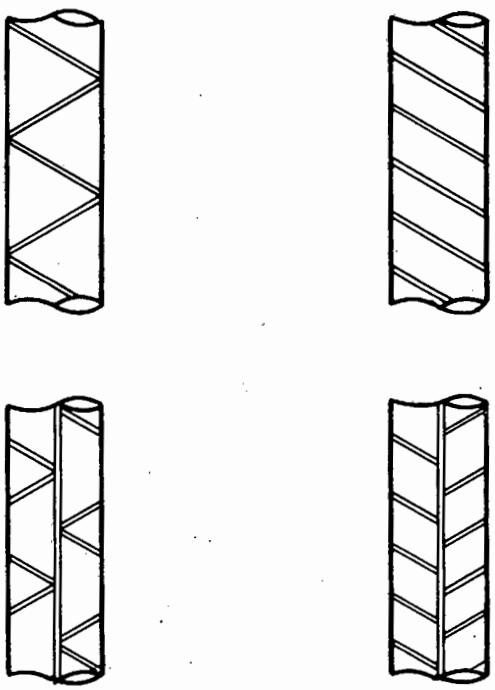

SINGLE HELICAL CROSSED

DOUBLE HELICAL STAGGERED.

Figure 11 : Common Shapes Of Deformation Pattern.

Also illustrated in Figure 13 are similar curves obtained from tests by Rostasy and Hognestad [9]. Their findings substantiate those of Fergusons. However, Lutz has observed that the bond strength is not directly proportional to the diameter unless the bar is confined by spirals. This allows the distress of the concrete keys to become a greater factor in the bond strength. The influence of the concrete keys will be discussed in the following section.

(c) Height of the Rib.

Increasing the height of the rib can cause a significant increase in the bond strength and slip resistance due to the reduction of the bearing pressure on the rib. However, Lutz [2] has found that this increase is much less than the relative increase in the rib height; 13% increase in bond strength resulted from 100% increase in the rib height.

In Figure 14 steel stress versus slip curves are illustrated for different bearing areas and heights of deformation. The curves illustrate the increase in steel stress with increase in height of deformation and further that the shape of the deformation pattern does not influence slip as much as the height of rib. There is no significant difference in stress for the different helical patterns illustrated which have the same height of deformation.

The relation between relative slip and rib height found by Rehm [5] is given in Figure 15. This relationship is based on his tests performed on single rib pullout specimens in which the rib was pulled opposite to the direction of settlement of the concrete during casting. Tests on ribs pulled in the direction of the concrete settlement would be different.

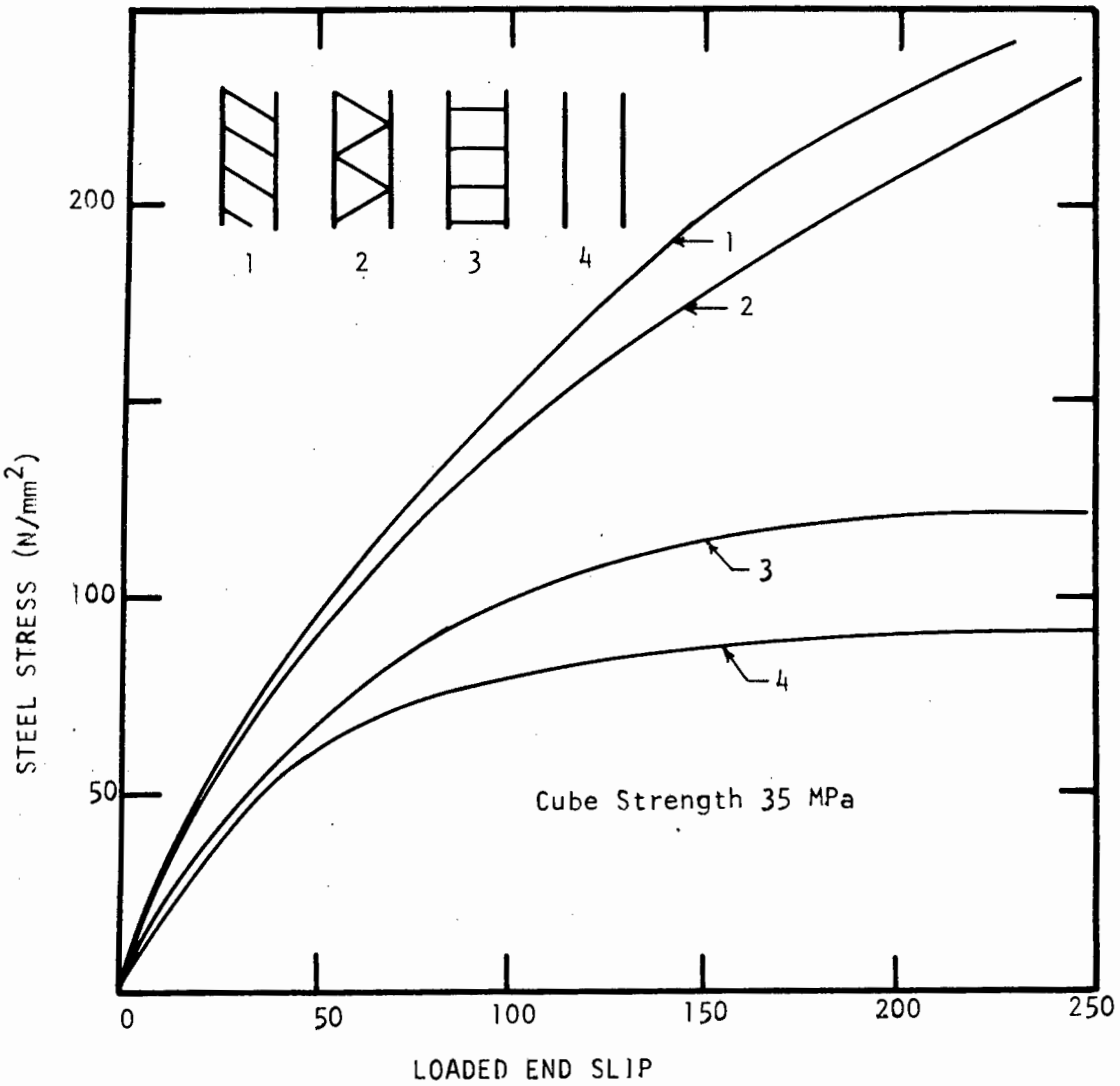

Figure 12 Steel Stress Versus Slip For Different Deformation Patterns (7)

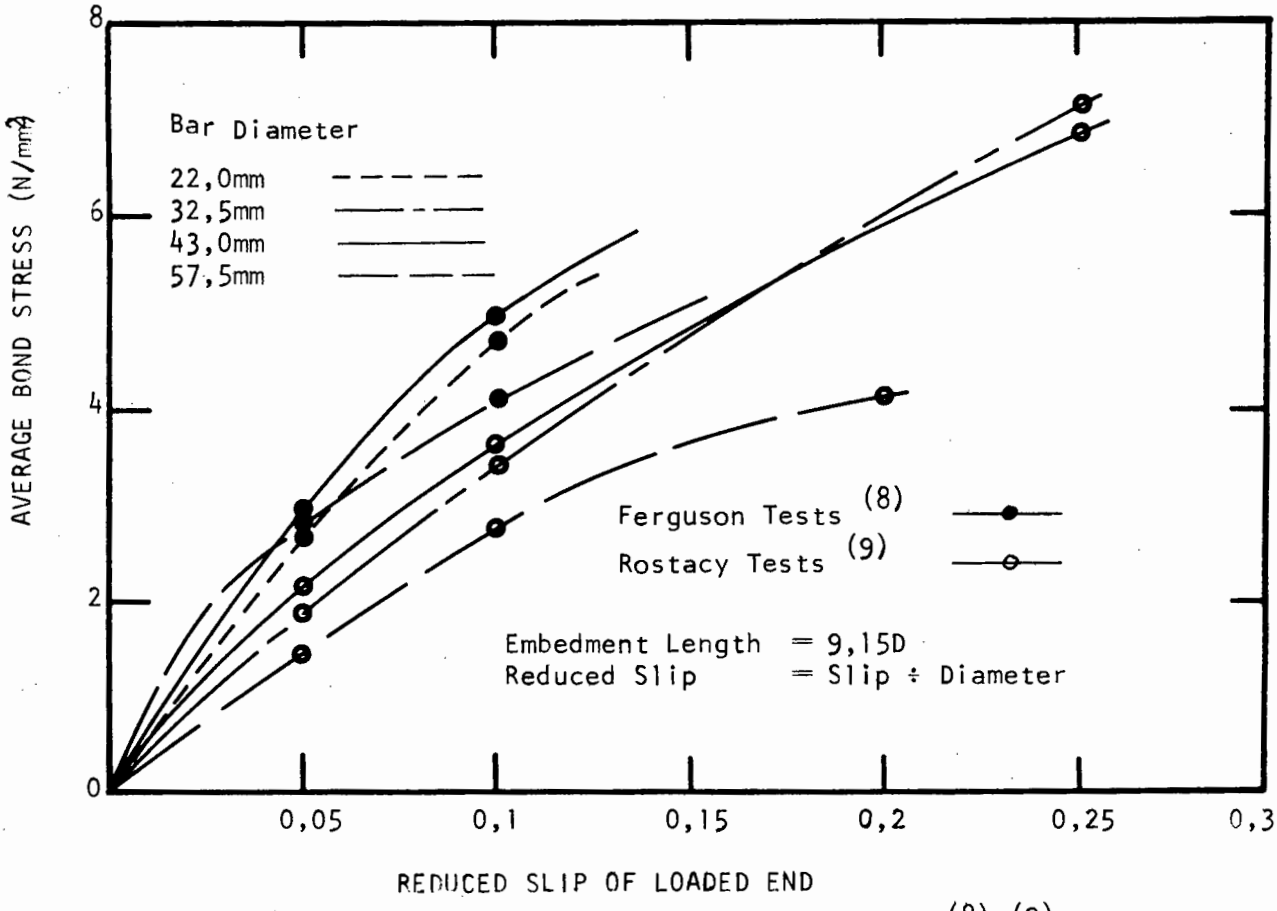

Figure 13 Bond Stress Versus Reduced Slip (8), (9)

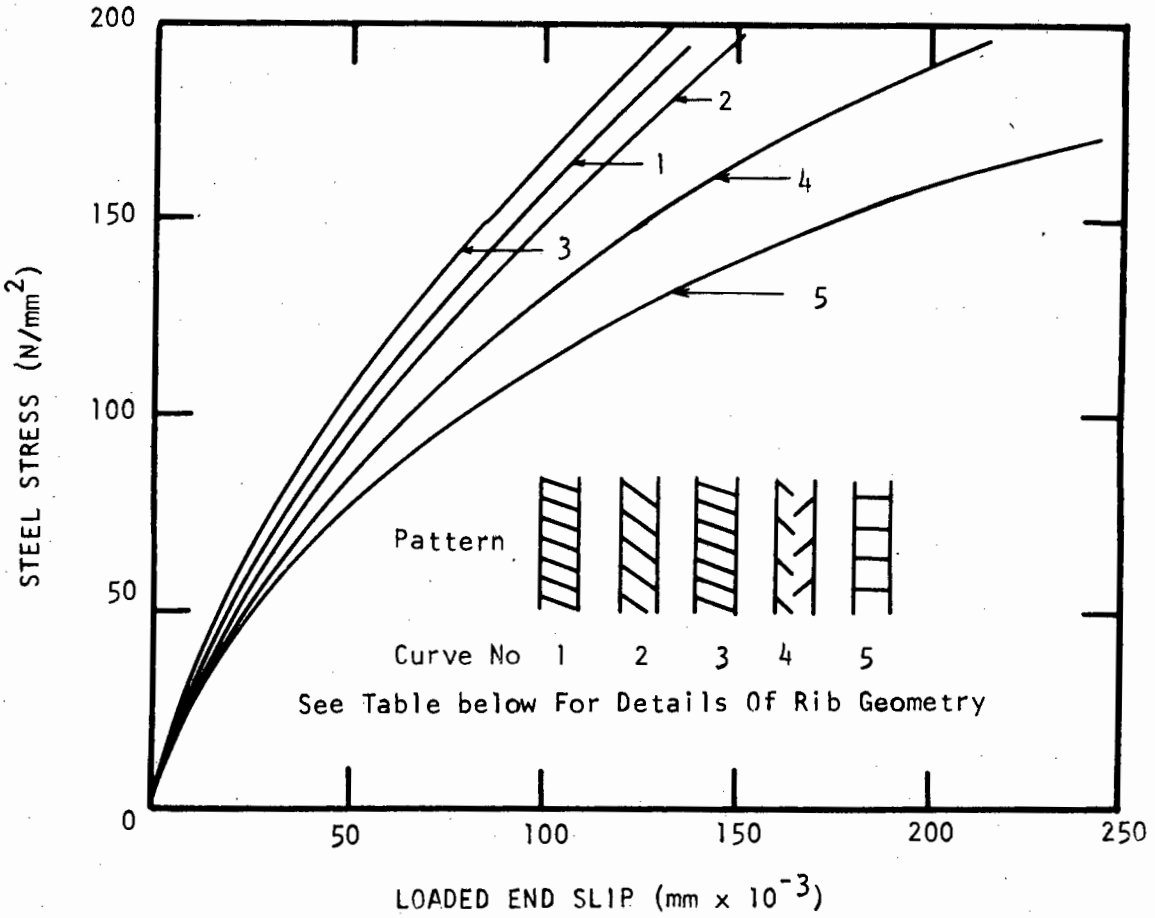

Figure 14 : Steel Stress Versus Slip For Different Heights Of Rib And Bearing Area [7].

DETAILS OF RIB GEOMETRY

Number of Curve	1	2	3	4	5
Height of Rib (mm)	1,398	1,270	1,398	0,710	0,833
Bearing Area of Rib for 10mm Length of Bar (mm^2)	93	65	100	26	10
Cube Strength 35 (N/mm^2)					

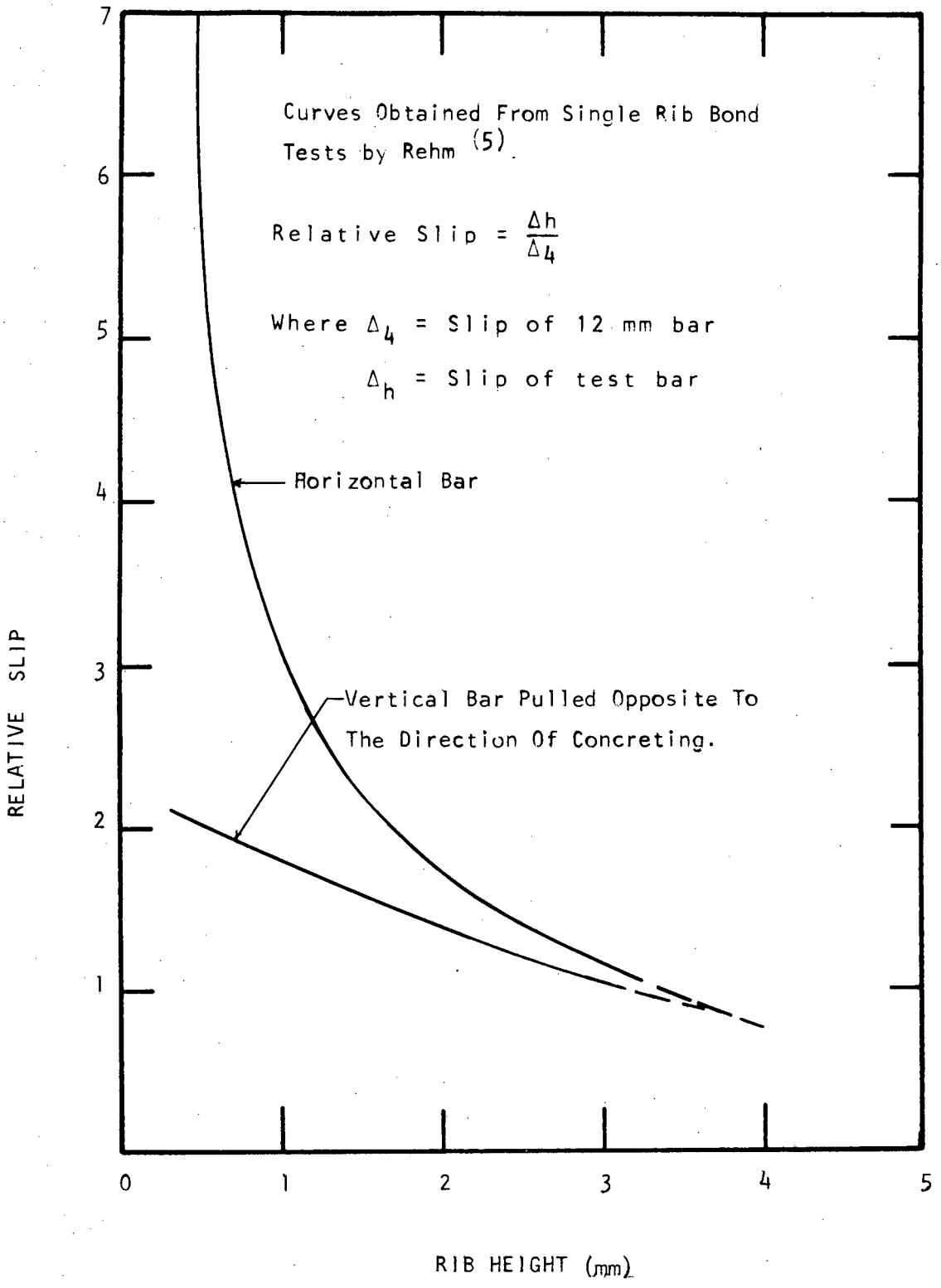

Figure 15 : The Influences Of Rib Height On The Slip For Equal Rib Load Per Unit Perimeter (5).

Clark [7] found that the slip resistance of top-cast bars (380 mm bottom cover) relative to that of bottom-cast bars (51 mm bottom cover) correlated directly with rib height. This indicates that the adverse effects of settlement and consequent water gain below a top-cast bar can be overcome to a large extent by increased rib height.

(d) Rib Spacing.

Considering a bar of given diameter embedded for a given length, the bearing pressure of the ribs may be reduced by increasing the rib heights and by increasing the number of ribs in this given length of bar. The area in shear increases with increasing rib height (outer bar diameter increases) and decreases somewhat with number of ribs (more rib widths existing on shear plane). Therefore, shear stresses can only be substantially reduced by improving the manner in which shear is transferred into the concrete. Rehm[5] determined that when the average shear stress becomes large, the concrete key will fail in a region with a length equal to 5 to 7 times the height of the rib. Thus for a given rib height the whole concrete key can be made effective by reducing the rib spacing so that failure occurs over the whole concrete key. Thus Rehm concluded that the failure plane would extend between adjacent ribs provided that the ratio

$$\frac{\text{clear rib spacing (c)}}{\text{rib height (h)}} < 7 \quad \text{(Figure 7)}$$

Lutz has found that improvements in bond strength and slip resistance can be obtained for $\frac{c}{h}$ as low as 1,33.

Tests of deformed bars with varying rib properties by Clark [7] show that improvement in the slip resistance correlates with the decreasing ratio of shearing area

to bearing area of the ribs i.e. approximately with the ratio of clear spacing between the ribs (c), and the height of the rib (h). As a result of this investigation, Clark considered a ratio of shearing to bearing area of 5 to 6 as desirable.

(e) Rib Face Angle.

The rib face angle also influences the bond properties of the deformed bars. Tests by Clark [7] and Rehm [5] indicate that the exact angle of the rib face is not too important as long as the angle of the rib face with the bar axis is 45 ^{o} or greater.

Rehm examined the characteristics of a single rib having various rib face angles. He found little difference between ribs with rib face angles between 45^{o} and 90^{o}. However, Rehm noted that the slip resistance of a bar with a rib face angle of 24^{o} was less than the others. This is attributed to the more gradual manner in which the load is transferred to the concrete. This finding was substantiated by Lutz who concluded that a rib with a face angle less than 30^{o}to 40^{o} will slip relative to the adjacent concrete, while ribs with a face angle of 40^{o} to 45^{o} achieve this slip by crushing of the concrete under the rib. Any rib with a face angle greater than 40 - 45^{o} will exhibit essentially the same slip characteristics.

(f) Rust and Scale.

Rust and scale primarily effect the friction and adhesion of reinforcing steel bars. Tests by Abrahams [10] using plain bars show that firm rust increases the bond resistance of these bars. This is because the bond of this type of reinforcing bar is very largely dependent on surface adhesion between the concrete and steel. Consequently, the presence of a roughened surface tends to increase the adhesion.

Extensive research on rusted deformed bars was performed by Johnston and Cox [12]. Their results indicate that:

(a) at low values of slip, higher bond stresses are developed by heavily rusted bars than by corresponding tests of unrusted bars,

(b) the total amount of slip attained before reaching ultimate bond strength is greater for unrusted or slightly rusted bars than for heavily rusted bars,

(c) the ultimate pullout strength of the bar is not greatly affected by the conditions of rust.

Recent research by Kemp et al [11] on rusted deformed bars has substantiated the conclusions of Johnston and Cox. Kemp's results are indicated in Figure 16 where average bond stress is plotted against slip of the loaded end of the bar. From the curves it is also concluded that the bar surface condition, for all but the artificial scale specimens, has little influence on the bond resistance. However, the initial slope of the bond-slip curve is affected slightly by surface conditions. Bars with slightly rusted surfaces produced less slip than those with a heavy rust.

(ii) Properties Of The Concrete.

(a) Compressive Strength.

The bearing stresses at the rib interface may become very large and consequently the compressive strength of the concrete will influence the bond strength of deformed bars. Lutz[2] determined that the average bearing stress on the rib of a 25,4 mm bar at ultimate failure is 372,0 N/mm^2. However, this value is not of

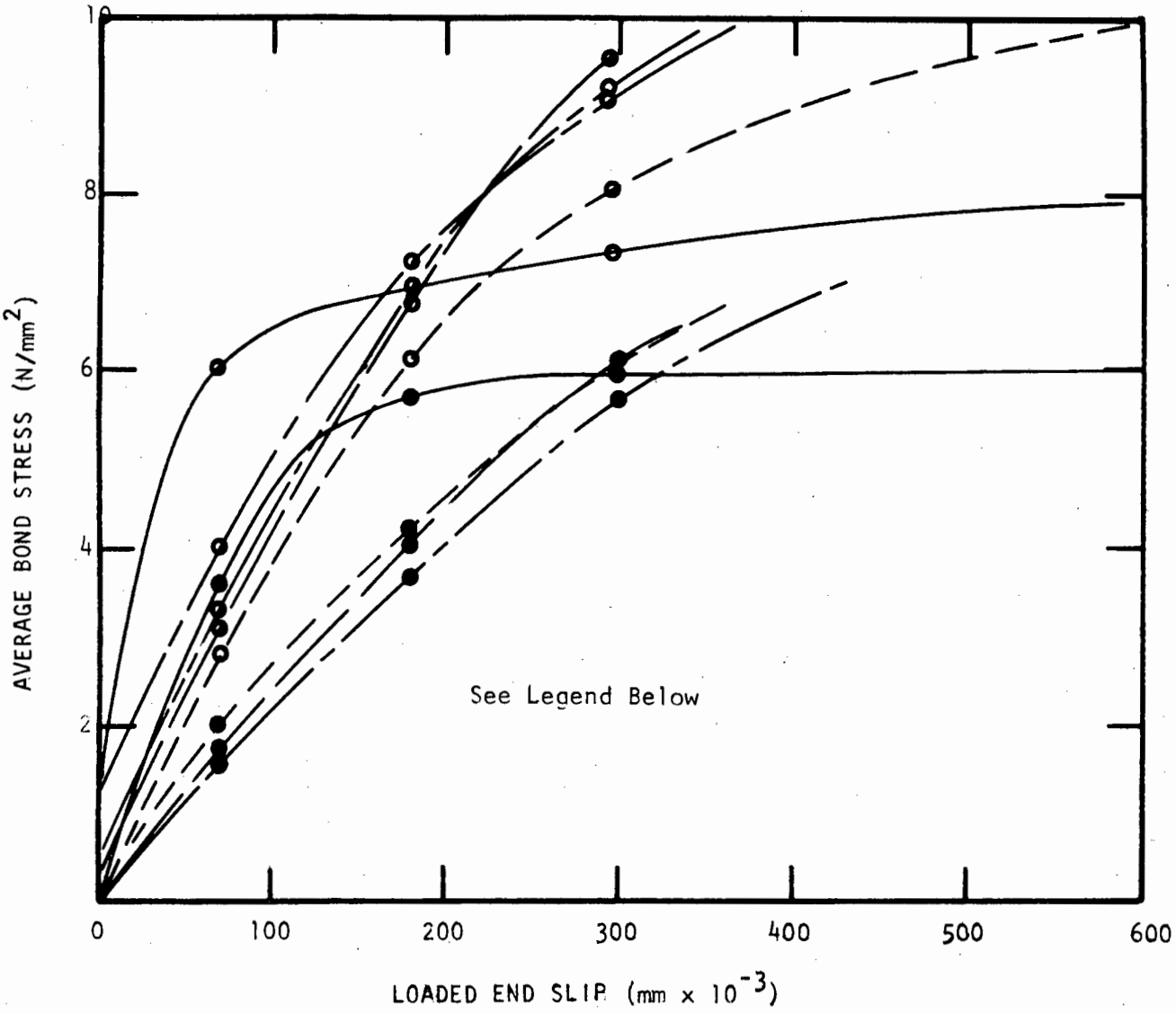

Figure 16 : Effect Of Different Surface Conditions On Loaded End Slip Of Deformed Bars[11]

12 mm Diam. Bar
29 mm Diam. Bar
Unrusted Bar
Air Rusted Bar
Fresh Water Rusted Bar
Salt Water Rusted Bar
Artificial Scale Bar
Cube Strength 23 N/mm^3

practical interest because bond stresses are limited to 1,50 N/mm^2 and the corresponding bearing stress is then about 82,0 N/mm^2 for 20,65 N/mm^2 concrete. Thus the local bearing stress on a rib at bond failure is about three times the compressive strength of the concrete.

The strength of the mortar in bearing is influenced by its moisture condition. Both Rehm [5] and Lutz [2] determined that a drier mortar can cause a higher bond resistance. This increase is due to the increase in compressive strength of dry mortar (20% to 30%) and also to a lesser extent on the better frictional properties of the drier interfacial surface.

The average bond strength of a reinforcing bar is linearly related to the cube compressive strength of the concrete. In Figure 17 average bond strength is plotted against cube compressive strength. It can be seen from these curves that the concrete mixes having higher compressive strengths exhibit higher bond strengths.

Rehm [5] examined the dependency of the bond-slip curves on the compressive strength. He determined that the slip resistance is proportional to the concrete strength at large values of slip. However, at low values of slip the resistance increases more approximately in proportion to the square root of the compressive strength.

Perry and Thompson [16] determined the influence of concrete strength on the distribution of bond stress. Their results for deformed bars are shown in Figure 18. From the figure it can be seen that for the same load the point of maximum bond stress is closer to the free end for mixes with low compressive strength. This point of maximum stress is just ahead of the propagation of the splitting crack.

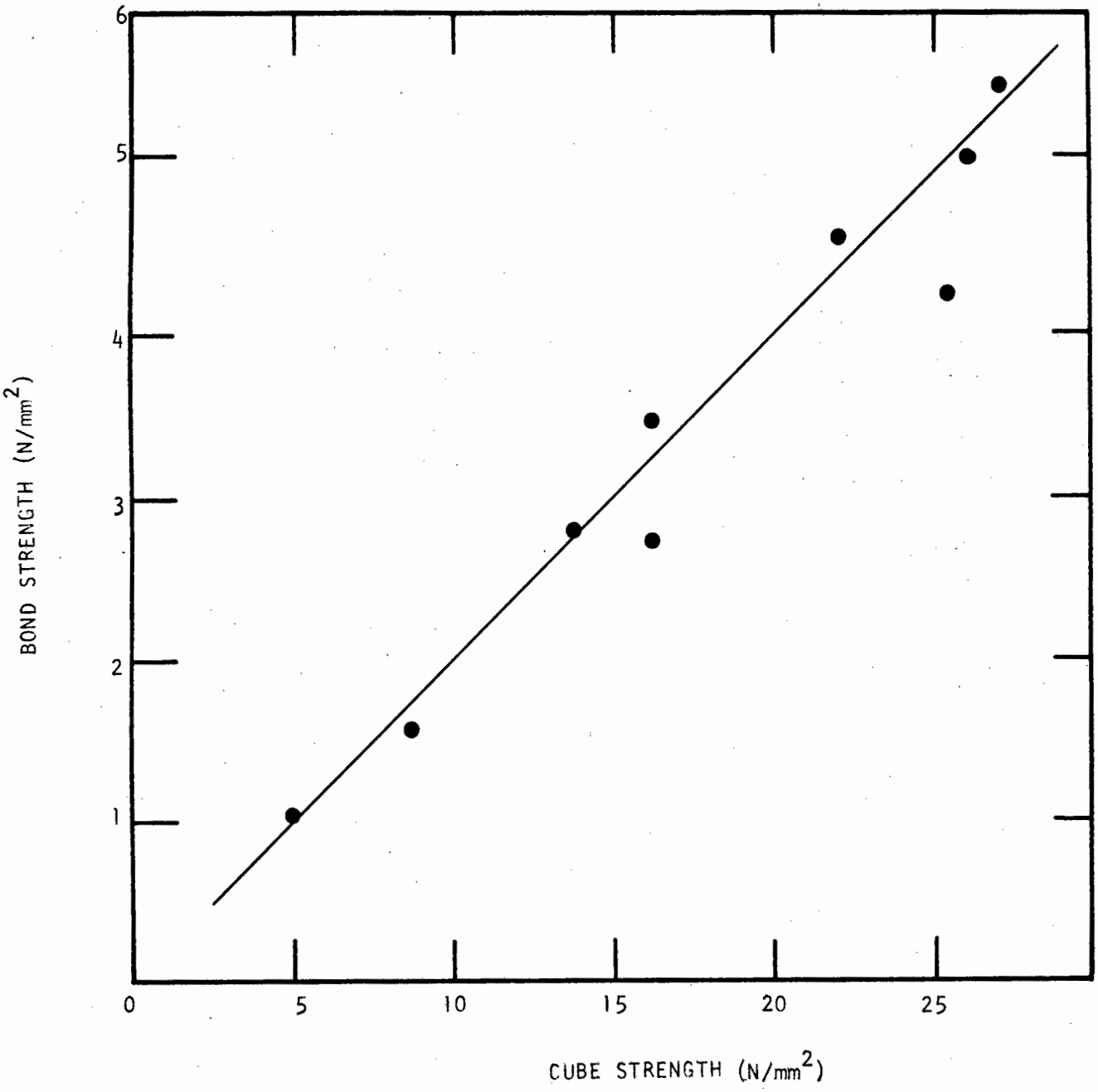

Figure 17 : Relation Between Average Bond Strength and Cube Compressive Strength Of Concrete [19]

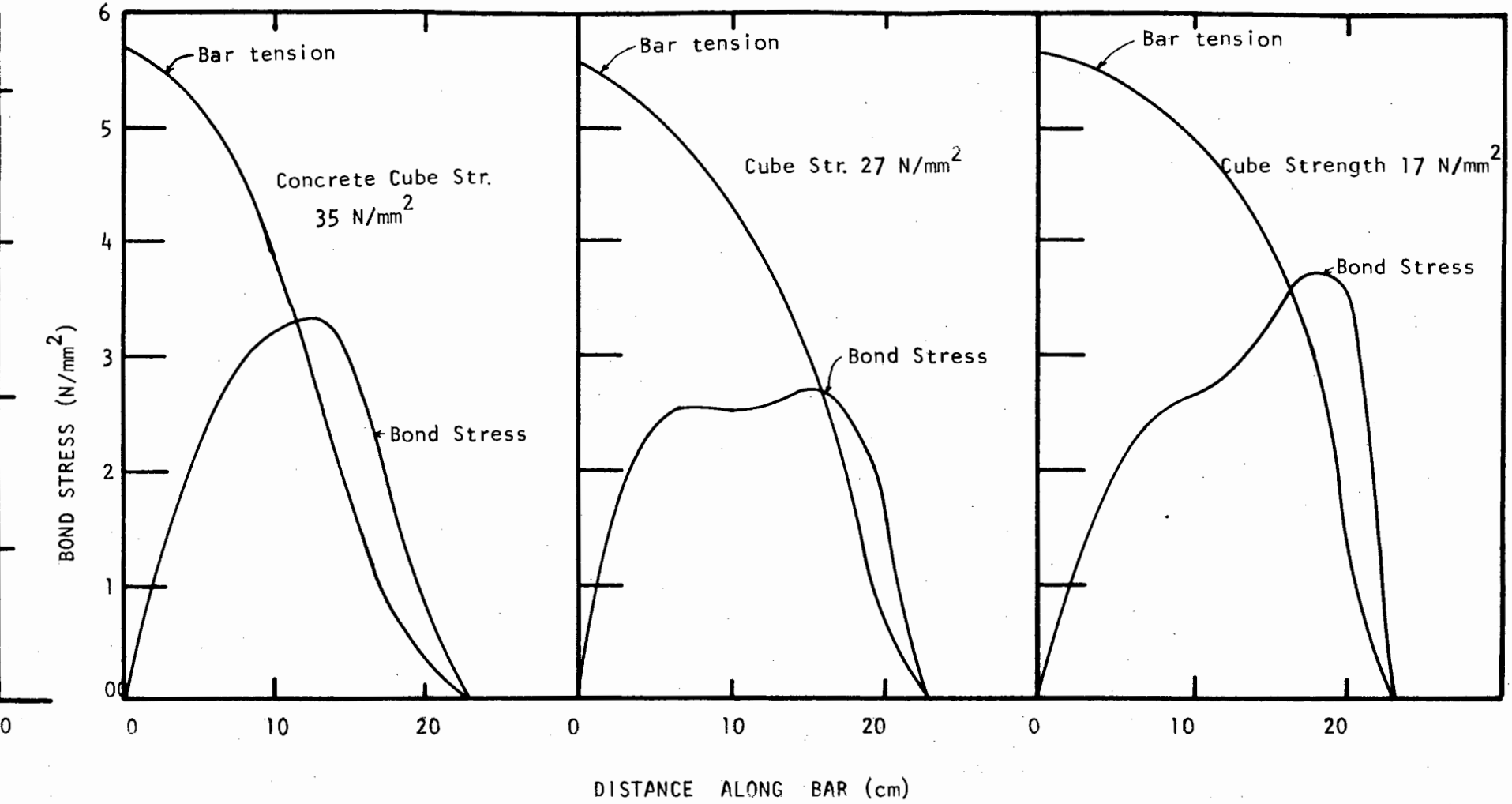

Figure 18 Effect Of Concrete Strength On Bar Tension And Bond Stress Of Eccentric Pullout Specimen (16)

(b) Tensile Strength.

The tensile strength of concrete affects the bond due to its influence on the development of cracks.

Tensile stresses are developed by shrinkage of the concrete surrounding the bar. These stresses can cause splitting (high circumferential stresses) or transverse cracks (longitudinal tensile stresses).

Subsequent loading of the reinforcing bar increases the longitudinal tensile stresses. After some transverse cracking has occurred, the stress distribution changes considerably. The longitudinal stresses in the concrete are reduced while the bar stresses are increased. The increased load on the bar in the vicinity of the crack causes large straining of the bar which forces the concrete to strain with the steel. Transverse cracking near the reinforcement is thus increased.

Cracking of the concrete controls the bond capacity adjacent to transverse cracks i.e. the bearing pressure or wedging action of the ribs is reduced because of the tensile forces produced in the concrete. Tests by Lutz[2] have indicated that wedging action cannot be fully developed in a distance of less than 1,5D from a transverse crack,

where D = diameter of reinforcing bar.

(c) Maturity of Concrete.

Plowman [17] has determined that the relationship between the average bond strength and log maturity is linear. This relation takes the form:

$$\left.\begin{array}{l}\text{Percentage of average bond}\\ \text{strength at maturity of } 35600^{\circ}\text{F.hr}\end{array}\right) = A + B \log_{10}\left(\frac{\text{MATURITY}}{10^3}\right)$$

The constants A and B vary linearly with bond strength and are readily calculated from graphs. (17)

Peattie and Pope (1) have shown that the development of bond strength occurs at a faster rate than the increase in compressive strength. This is attributed to the rapid shrinkage of concrete in its initial stages of maturity.

In Figure 19 bond stress and compressive strength are respectively plotted against the age of concrete in days. The results of Peattie and Pope illustrated in this diagram, indicate that bond strength attains its ultimate value after approximately five days, whereas compressive strength attains its ultimate value only after many years. Also shown in Figure 19 is the bond strength versus age of concrete in days as determined by equation 1. The bond strength continues to increase even after 28 days. The parameters in both investigations are identical except for the surface condition of the bars. Peattie and Pope used plain machined bars whereas Plowman performed his tests using plain bars in the rolled condition and, as such, would be rougher than the machined bars. The rougher bars appear to be more dependent on the compressive strength, than on the shrinkage of the concrete, whereas the polished bars are influenced by shrinkage only.

(d) Workability of the Concrete.

It is difficult to isolate the effect workability exerts on bond because the position of the bar during casting influences the results. This is illustrated by the results of Clark (14) shown in Figure 20. In this diagram bond stress is plotted against slip for bars cast in the top horizontal, bottom horizontal, and vertical positions respectively. The concrete had slumps of 88,9 mm and 147 mm. It is apparent that for bars cast in the top horizontal or vertical positions, the low slump mix exhibits higher bond stresses at a particular slip than the mix of higher slump. However, for bars

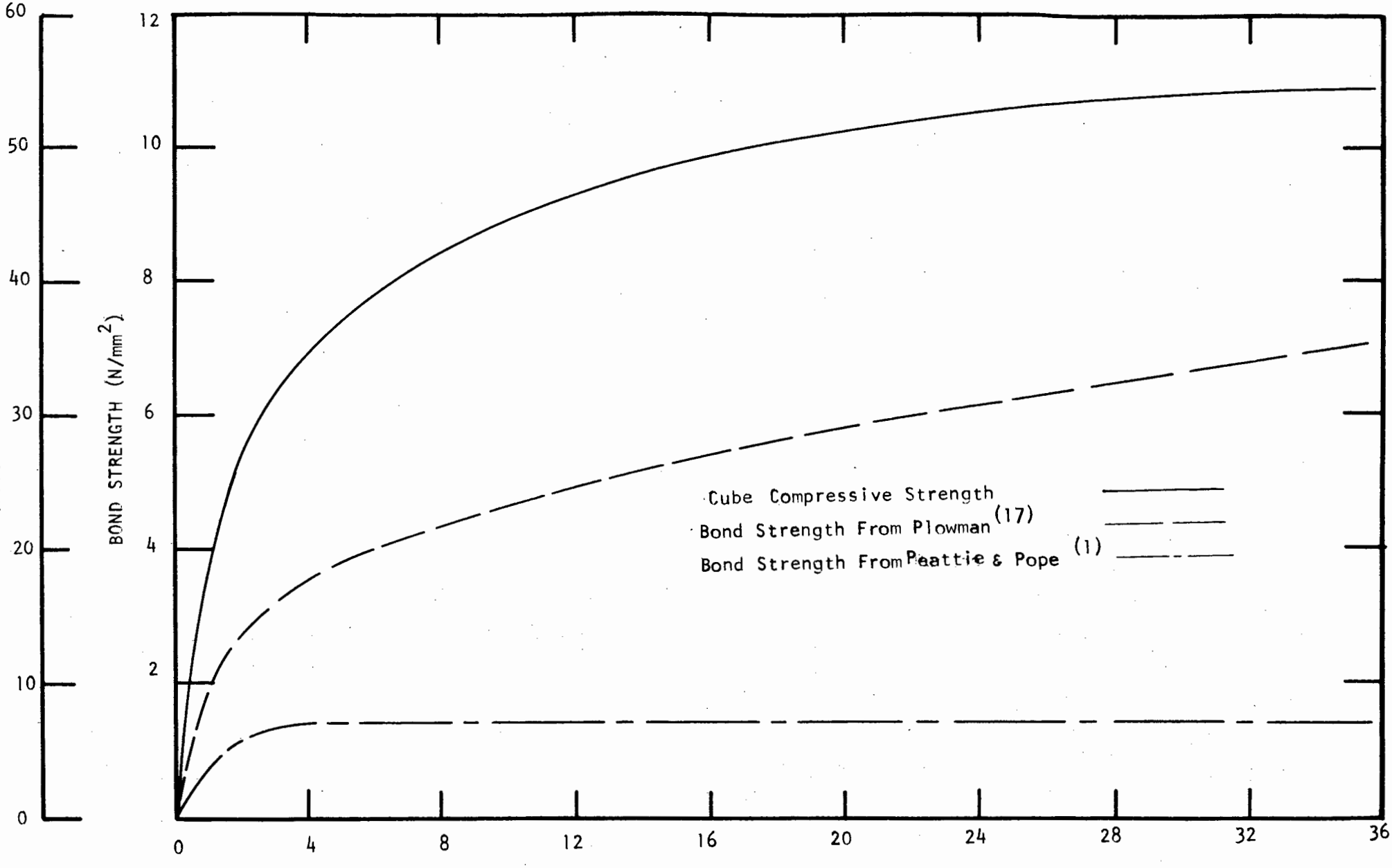

Figure 19 : Compressive Strength And Bond Strength Development With Age (1), (17)

cast in the bottom horizontal position the converse is true, i.e. the high slump mix has higher bond stresses at a particular slip than the low slump mix. This difference in slip resistance of bottom and top cast bars is attributed to the greater settlement of the concrete beneath the top cast bar than beneath the bottom cast bar.

(iii) Embedment Length.

Bond stresses are found to be more uniform along the lengths of bars with short embedment lengths than those with long embedment lengths [7]. In this respect it should be noted that bond stresses developed by frictional effects are more uniform than those due to chemical adhesion and mechanical interaction. Consequently, the bond stresses of plain bars will vary greatly for long lengths of embedment i.e. when all three bond mechanisms are effective. In Figure 21 bond stress versus distance from the loaded end is illustrated for embedment lengths of 203,3 mm and 305 mm respectively. It is apparent that the bond stress for an applied load of 26,7 kN varies more in the 305 mm embedment length bars than in the 203 mm embedment length bars.

Average bond stress at a given loaded end slip decreases rapidly as length of embedment is increased. This is clearly illustrated in Figure 22 where average bond stress versus loaded end slip is plotted. The variation of average bond stress with length of embedment reflects the fact that the bond stresses tend to concentrate at the loaded end.

(iv) Casting Position Of Reinforcing Bar.

The following factors with regard to the casting position of the reinforcing bar influence its slip resistance:

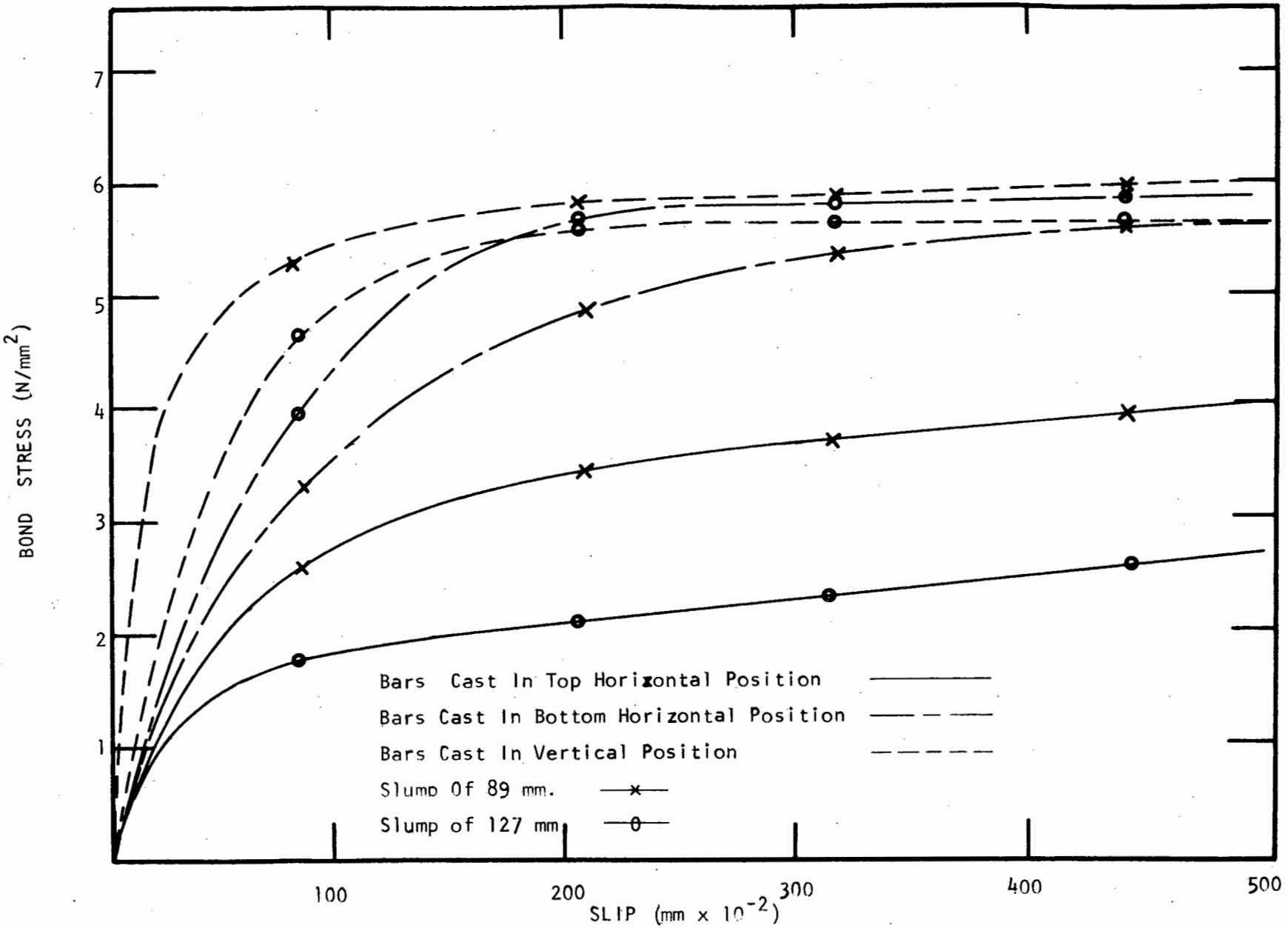

Figure 20: The Effect Of Slump On The Bond Strength For Different Casting Positions Of Bar [14]

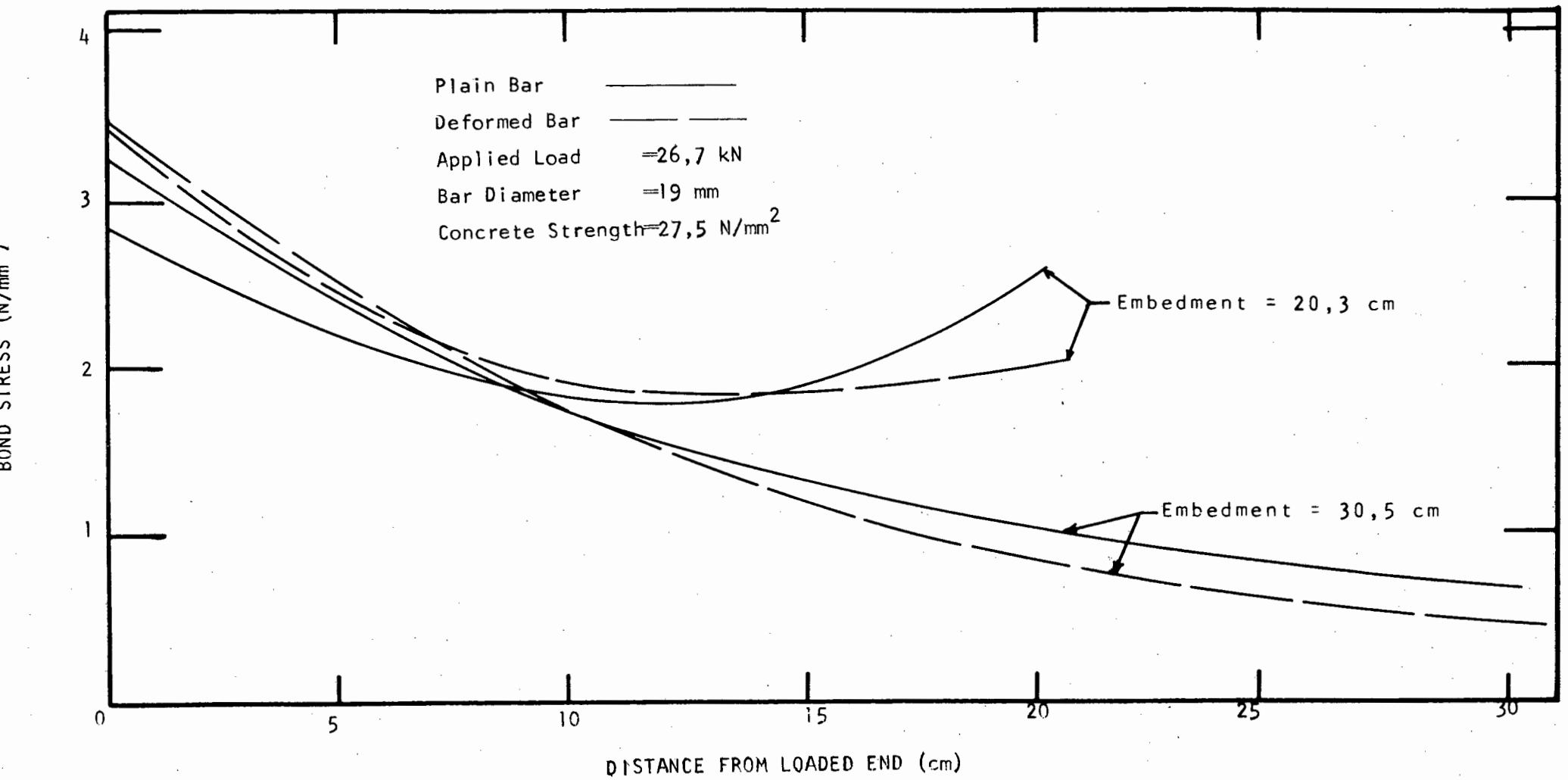

Figure 21 Distribution Of Bond Stress In Pullout Specimens (6)

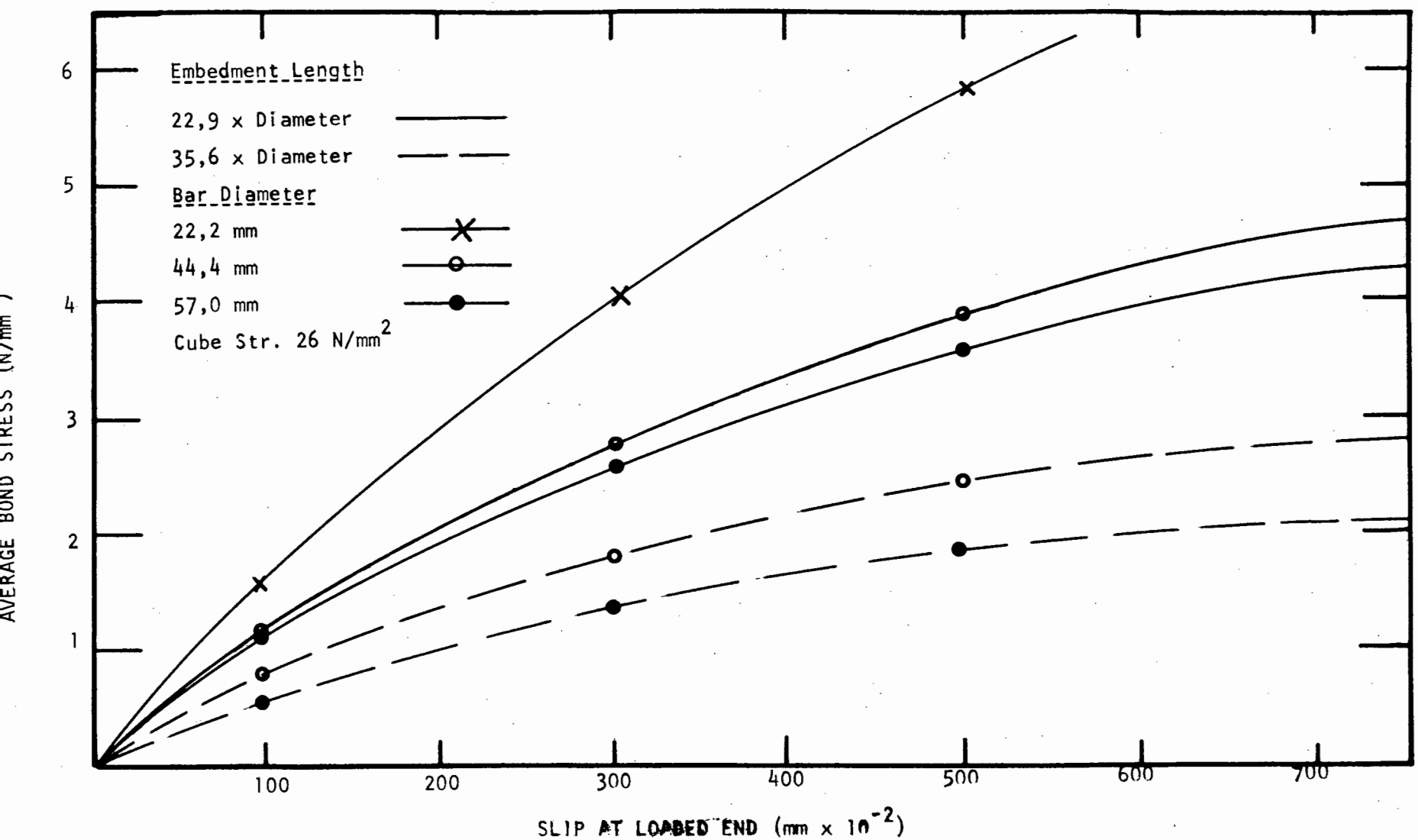

Figure 22: Average Bond Stress For Different Lengths Of Embedment (8)

(a) bar orientation i.e. vertical or horizontal casting position

(b) depth of concrete below a horizontally cast bar

(c) direction of load application relative to settlement of concrete with bar cast in the vertical position.

Rehm [4] examined the slip resistance of horizontally placed bars relative to that of vertically placed bars. The bars cast in the vertical position were loaded opposite to the direction of settlement of the concrete. He found that for single rib bars the ratio of relative compression, X_R, (vide page 16) of horizontally placed bars to vertically placed bars, varies from about 0,3 for a rib height of 0,5 mm to 1 for a rib height of 4 mm. In Figure 23 the relative compression versus slip is plotted for horizontally cast bars and vertically cast bars subjected to tension opposite to the direction of concreting and also vertically placed bars subjected to tension in the direction of concreting. The rapid increase in relative compression after slip of about 0,01 mm for the bar loaded in the direction of concreting indicates that a porous layer of mortar is present under the rib and that this layer is rapidly compacted as the slip becomes greater.

Clark [14] concluded from the results of his tests, shown in Figure 20, that top-cast bars are two thirds as effective as the corresponding bottom-cast bars. This decrease in slip resistance of top-cast bars is due to the greater settlement of concrete beneath these bars than beneath bottom-cast bars. (vide page 27)

(v) Temperature.

Very little research has been directed towards determining the effect of temperature on the bond between concrete and

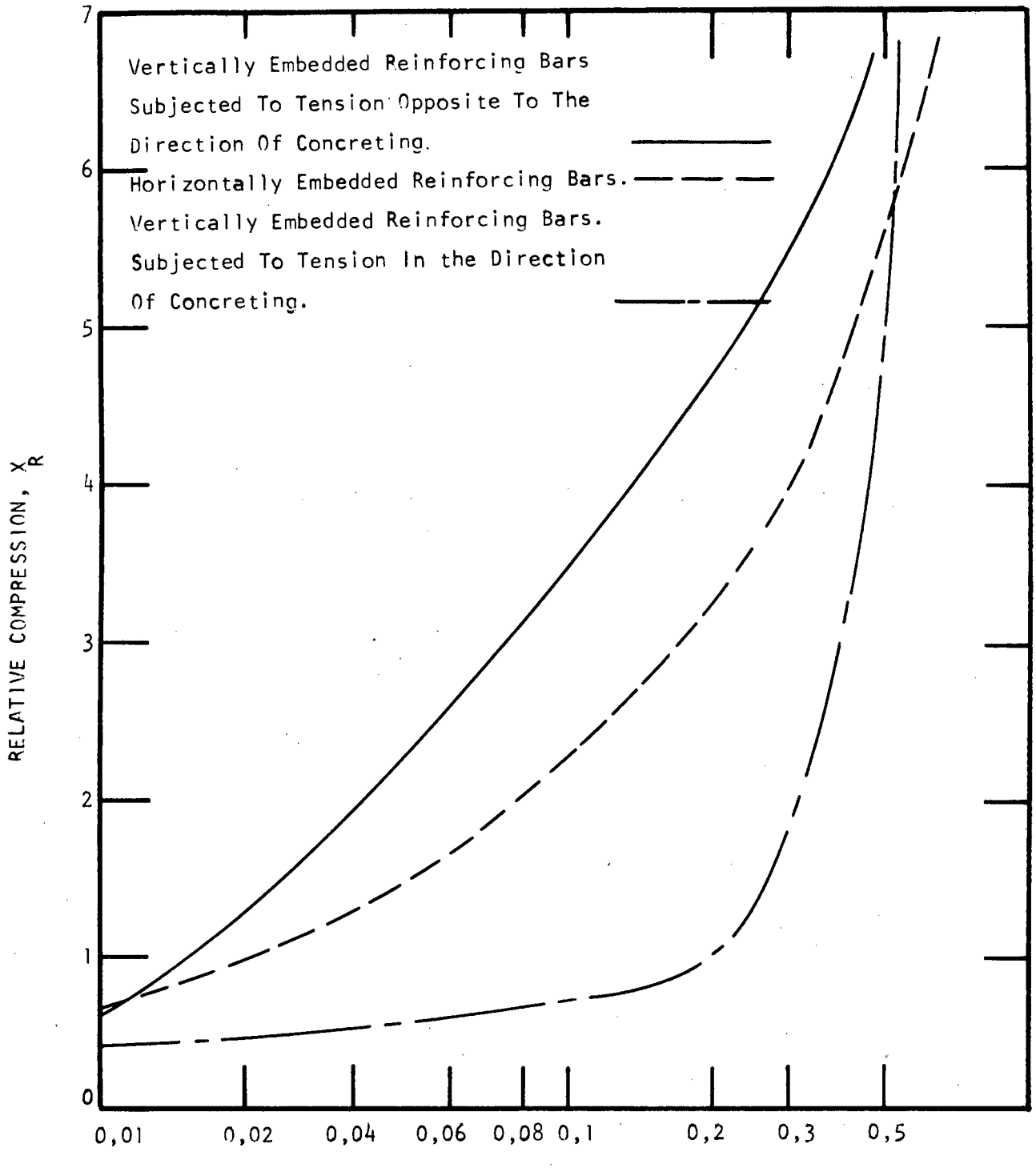

Figure 23 : Effect Of Bar Orientation On The Rib Bearing Stress Versus Slip Curves[4].

reinforcing steel.

Harada et al [20] performed pullout tests to study the effect on bond of temperatures up to 400°C. The 150 mm diameter cylindrical specimens were slowly heated for 10 hours to temperatures of 110°C, 300°C and 450°C respectively. After maintaining the temperature for three days the specimens were gradually cooled and the bond strength tests performed in accordance with ASTM C234-57T [21].

The residual ratio of bond stress versus temperature is shown in Figure 24. From this diagram it can be seen that the bond stress decreases rapidly with increase in temperature - at 300°C the bond being reduced to 50 per cent of the unheated value.

It is interesting to note that the decrease of residual bond stress between 100°C - 300°C is only 5%. This is due to the increase in compressive and tensile strength of concrete at these temperatures. The effect of temperature on the strength of concrete will be fully covered in Chapter Four. (vide page 68)

Summary.

Factors which affect bond are numerous. Consequently, the results of different investigators are occasionally conflicting.

The geometry of the rib is the property of the reinforcing bar which has the greatest affect on the bond resistance. Increasing the rib height and rib face angle increases the bond. However, increasing the rib face angle above 45° produces no significant increase in bond. Reducing the rib spacing to $\frac{c}{h}$ ratios of 5-7, ensures that shear failure occurs over the whole concrete key. Bar diameter and deformation pattern do not influence bond to the same extent as the rib geometry. Greater slips are produced by larger diameter bars - slip varying approximately in

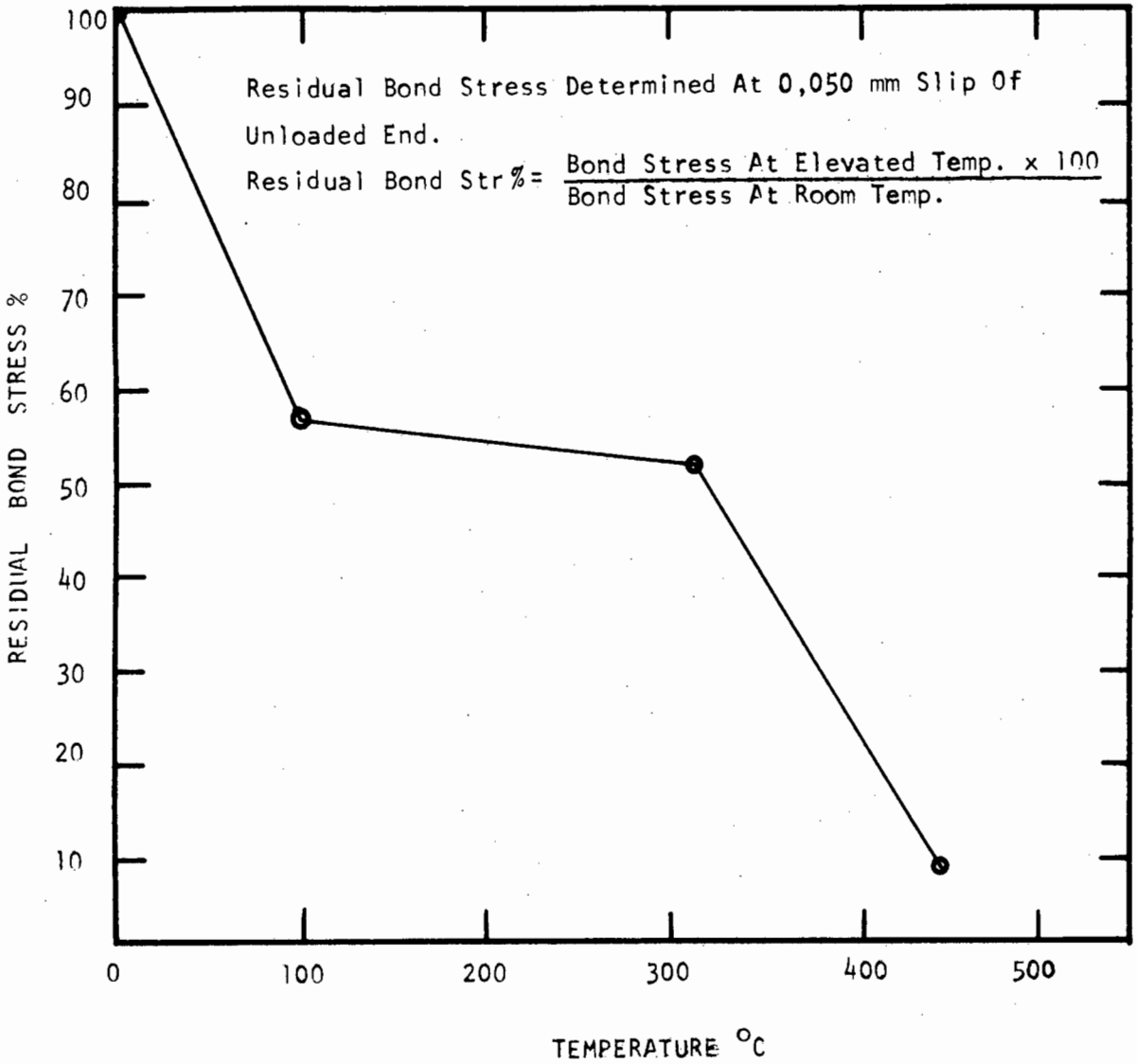

Figure 24 : The Effect Of Temperature On Residual Bond Stress At 0,050 mm Slip Of Unloaded End.

proportion to the diameter. Rust and scale primarily affect the bond of plain bars - the bond is increased by the roughened surface. The bond of deformed bars is increased at low loads by rust.

Bond is dependent upon the compressive and tensile strength of the concrete. Increases in compressive strength produce substantial increases in bond resistance. This is particularly the case for deformed bars where slip occurs by crushing of the concrete. The tensile strength of concrete is important in resisting the development of cracks. It has been shown that the bond capacity of the reinforcing bar is not fully developed in the distance of less than 1,5 diameters from a crack.

The relationship between bond strength and log maturity is linear. This relationship for plain bars is dependent upon the bar surface - machined bar surfaces attain a constant bond strength value at five days, whereas the 'as rolled' bar surface increases its bond strength even after twenty eight days.

The effect of workability on bond resistance is influenced by the casting position of the bar. Bars cast in the top horizontal position have the greatest slip, particularly when high slump mixes are used.

Temperature has been shown to decrease the bond strength. At 300^{o}C the reduction in bond strength is 50 per cent.

CHAPTER 3 - EXPERIMENTAL INVESTIGATION.

3.1) Materials.

(i) Steel.

The steel used was of local manufacture and was ordered in lengths of 1 metre. Prior to use both ends of the bars were machined to provide smooth bearing surfaces for the dial gauges.

Two types of reinforcing bars were used viz.:

(i) plain mild steel bars, and
(ii) high tensile steel bars having the deformation pattern illustrated in Figure 25.

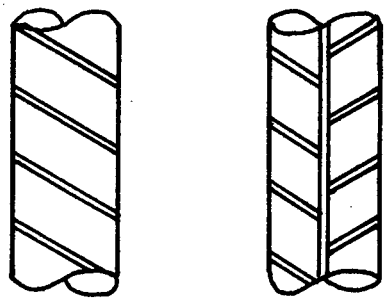

Figure 25. Staggered, Single, Helical Deformation Pattern.

The physical properties of the reinforcing bars used in this project are indicated in Table I. These results are the average values obtained from tests on six different bars (vide Appendix 2.1). The nominal diameter of the deformed bars was determined by weight and length measurements. The height of the ribs was determined by a purpose made jig.

TABLE I

	TYPE OF BAR			
Properties	Plain	Plain	Deformed	Deformed
Diameter (mm)	12,10	25,38	11,83	24,97
Area (mm^2)	114,98	505,87	109,89	489,66
Ht of Rib (h) (mm)	-	-	0,76	1,25
Rib Spacing (c) (mm)	-	-	4,9	14,9
c/h	-	-	7	12
Young's Mod (MPa)	206,63	206,32	201,10	202,48
Yield Str. (kN)	43,52	144,48	55,96	-
Ult. Tensile. Str. (kN)	61,97	232,15	88,72	400,48

Tensile steel tests were performed in the laboratory in accordance with SABS. The Young's Modulus and tensile strengths of the steel as found from these tests are also given in Table I.

(ii) Cement.

Ordinary Portland Cement was used in this investigation. The cement was purchased in two lots and stored in air-tight steel containers in the laboratory to prevent the absorption of moisture.

A chemical analysis and physical property determination of the cement was performed in accordance with SABS 471 - both at the beginning and at the end of the experimental investigation. Results of these tests* may be found in Appendix 2.2. No significant differences in the properties of the cement are apparent.

(iii) Aggregates.

Fine Aggregate.

The fine aggregate was a Cape Flats sand having a specific

*Tests by National Portland Cement Company, Limited, Philippi, Cape.

gravity of 2,65 and fineness modulus of 1,98. The sand was dried prior to use and stored in metal containers in the laboratory. A grading analysis of the fine aggregate is given in Appendix 2.3.

Coarse Aggregate.

The coarse aggregate was a crushed quartzite having a specific gravity of 2,71 and a rodded bulk density of 1554 kg/m^3. The fraction of the coarse aggregate used was that passing a 12,5 mm but retained on a 4,2 mm mesh sieve. A typical grading analysis is given in Appendix 2.3. The coarse aggregate was washed and dried in the laboratory before use.

3.2 Manufacture Of Test Specimens.

(i) Test Specimen.

A cylindrical pullout specimen (250 mm diameter and 305 mm length) was used in preference to a beam specimen because of the ease of handling a pullout specimen when heated. A test specimen is diagramatically illustrated in Figure 26. The specimens were cast with reinforcing bars positioned vertically. The bearing surface of the specimens was cast against the machined bottom plate of the specially manufactured cast iron mould. During the bond strength test, the load was applied in the direction of concreting.

Preliminary tests indicated that spalling of the concrete surface occurred in the vicinity of the bar at the loaded end. This prevented accurate determination of the loaded end slip. Consequently, the test specimen was designed to have no bond for 100 mm from the loaded end. This was achieved by entwining the bars with greased string which was subsequently removed after the specimens had been stripped.

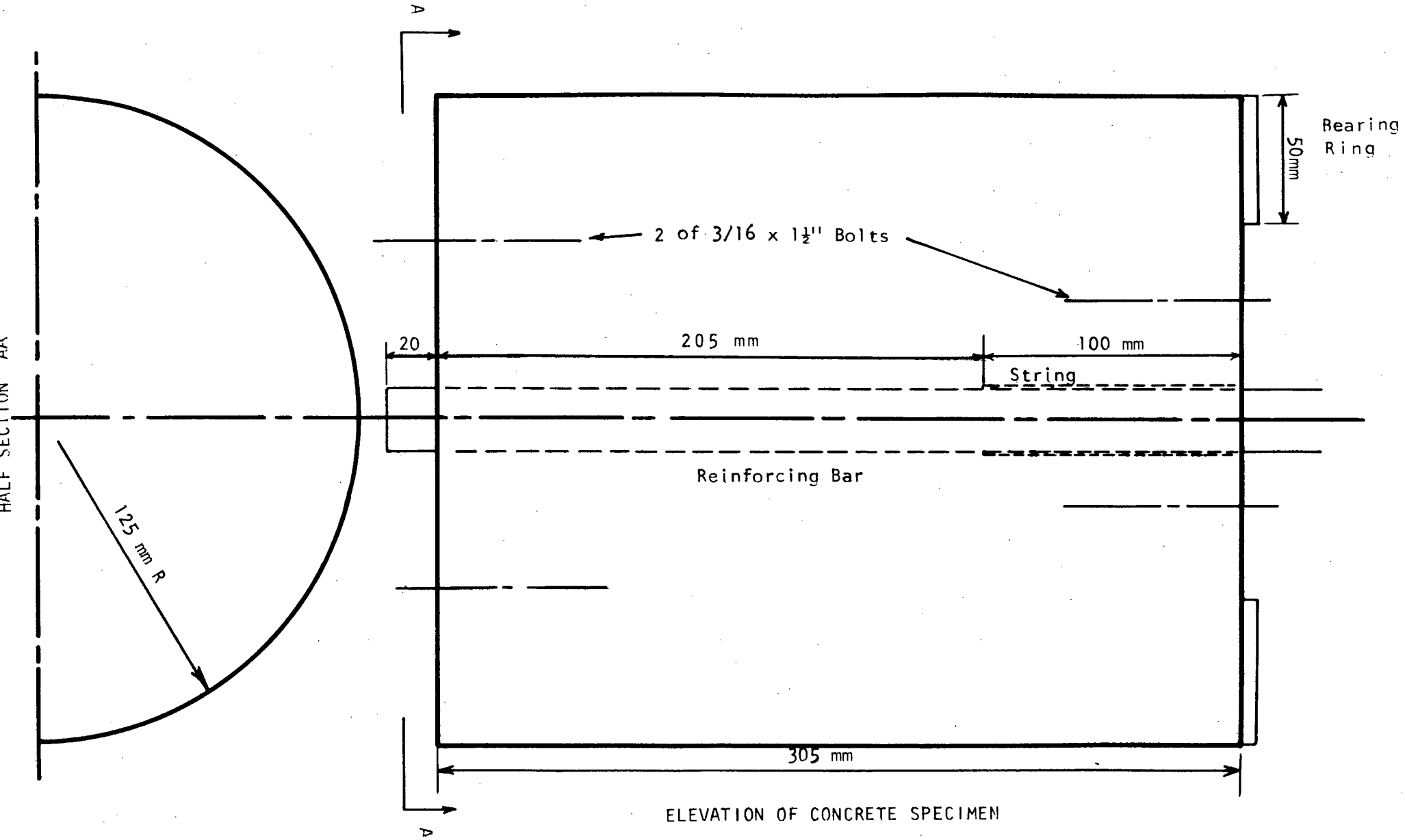

Figure 26: Detail of Test Specimen

The bars were held in position whilst casting by locating them through interchangeable inserts in the base plates. The holes through the inserts had diameters of 13 mm or 26 mm respectively, giving a tolerance of + 0,5 mm on the bar diameter. A typical insert is indicated in Figure 27.

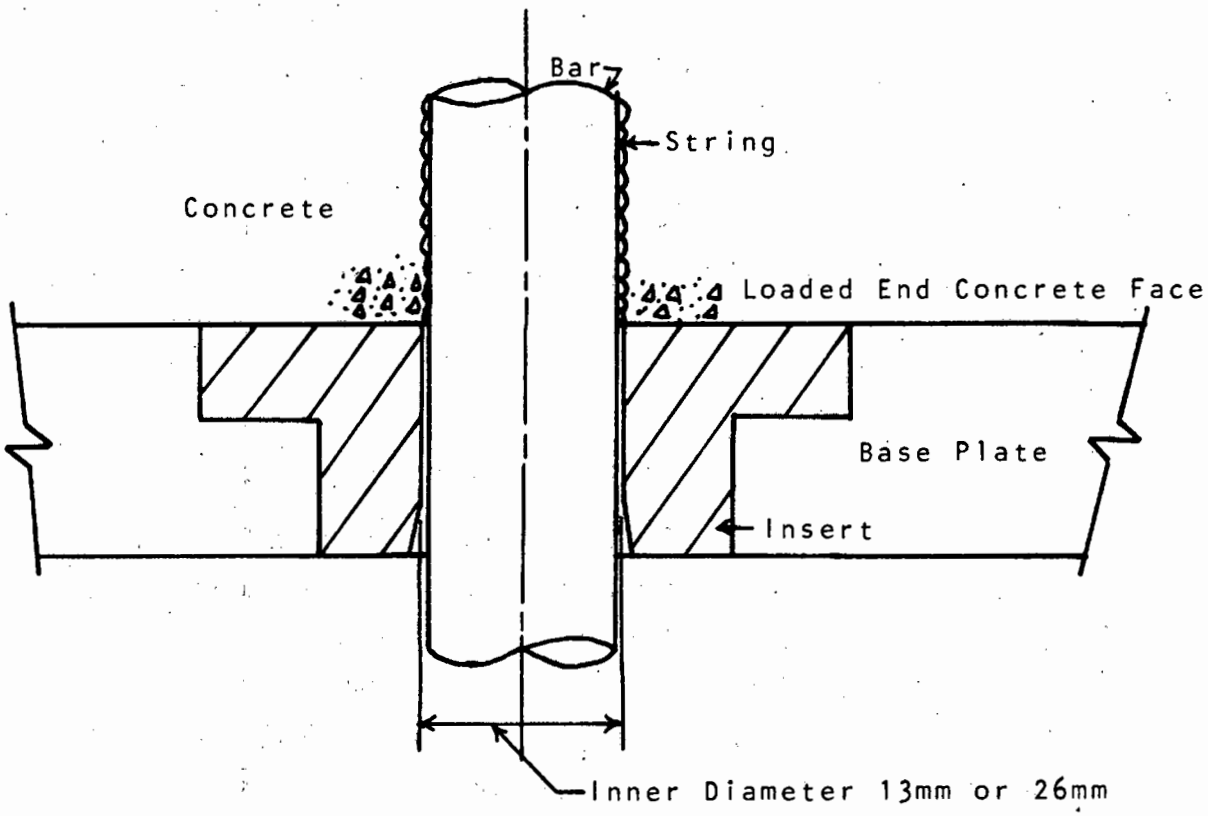

Figure 27. Insert In Base Plate For Locating Bar In Mould.

After casting, the unloaded end of the bar was located by measurement to within 1 mm of the specimen axis. The perpendicularity of the bar to the loaded end concrete surface thus fell within the limits set by the ASTM [22] - i.e. 0,5 degrees off the vertical or 3,175 mm in 305 mm.

Since the bars were found to exhibit different degrees of rusting, all bars used in this investigation were cleaned of rust and scale prior to casting. A steel brush was used for this purpose.

determined from the normal distribution graphs presented in Appendix 2.5 and are shown in Table III as well.

(iii) Curing of the Test Specimens.

The bond test specimens were cured for 24 hours in the moulds. The 150 mm cube cast with each batch was cured for 24 hours under moist hessian sacking. Bond specimens and cube were then stripped, care being taken not to break the bond (particularly of plain bar specimens) by rough handling. Final curing was under water at 23 $\pm$ 1°C for 28 days.

(iv) Casting and Testing Programme.

The nomenclature defining the different sets of specimens is read as follows:

All specimens have three symbols to identify them, e.g.

M1 • D • 25

First Symbol: This applies to the concrete mix used in the set of specimens.

- M1 - refers to the mix having water / cement ratio of 0,44 and Compacting Factor of 0,92.
- M2 - refers to the mix having water / cement ratio of 0,44 and Compacting Factor of 0,83.
- M3 - refers to the mix having water / cement ratio of 0,60 and Compacting Factor of 0,92.
- M4 - refers to the mix having water / cement ratio of 0,60 and Compacting Factor of 0,83.

Second Symbol: This applies to the type of deformation pattern on the reinforcing bar:

- D - refers to high tensile steel deformed bar.
- P - refers to plain mild steel bars.

Third Symbol: This refers to the nominal diameter of the bar: 12 mm or 25 mm bar.

The temperatures at which the bond tests were performed are: room temperature, 70°C, 110°C, 160°C, 250°C and 350°C. The complete testing programme followed in this investigation is given in Appendix 3.1

The casting and testing programme was divided into two sections. The first section completed tests at temperatures of 70°C, 160°C and 350°C. In this section two or three specimens were tested on each day. A two specimen batch was used for tests at room temperature and 350°C and batches of three specimens tested at room temperature, 70°C and 160°C. In the second section batches of three specimens per day were tested at room temperature, 110°C and 250°C.

The testing programme was planned by varying randomly the test parameters which included temperature, mix proportions, bar type and bar diameters in a cyclic order. Each cycle of tests was repeated three times.

3.3) Testing Procedures And Methods.

i) Bond Strength Pullout Tests.

The bond strength tests were performed in a 'beam and poise' testing machine (vide Appendix 2.6).

The test specimen was seated on a spherical bearing unit as illustrated in Figure 27. The bearing plate fitted into the movable head H_1 and the reinforcing bar was held by the stationary head H_2.*

* Preliminary tests indicated that the head, H_2, displaced slightly under the application of load.

Positions of the dial gauges are illustrated in Figure 27. The unloaded end slip was determined by dial gauge 1 which was mounted in a jig bolted to the concrete after heating. Readings of the unloaded end slip were estimated correct to 0,001 mm. The loaded end slip is determined as the average of the readings of gauges 2 and 3. These gauges bore on flanges welded to a pipe which fitted closely over the bar. The pipe was firmly held against the loaded end concrete surface by two springs attached to bolts cast into the concrete (vide page 57). Loaded end slip readings were read correct to 0,01 mm. Dial gauges 4 and 5 measured the relative movement between the movable head H1 and the stationary head H2. Dial gauge 5 was located on the end of the bar protruding through the jaws of the stationary head H2. The reading of the loaded end slip could accordingly be corrected for movement of H2.

The test specimen was loaded to an initial load of 2,224 kN. The dial gauges were then located and initial readings taken. Load was applied at increments of approximately one tenth of the estimated ultimate load. Slip readings were thus taken at 2,224 kN increments for the 12 mm plain bar, at 4,448 kN increments for the 25 mm plain bar and 12 mm deformed bar, and at 22,24 kN increments for the 25 mm deformed bar. To obtain the load-slip characteristics of the 25 mm deformed bar at loads below 44,48 kN, intermediate readings were ascertained at loads of 13,33 kN and 31,16 kN respectively.

ii) Heating of Test Specimens.

The test specimens were heated to the required temperature in specially designed cylindrical heating jackets (vide Appendix 2.6), firmly bound to the concrete by circular galvanised steel strips. The ends of the specimens were insulated during heating by 12 mm thick asbestos plates.

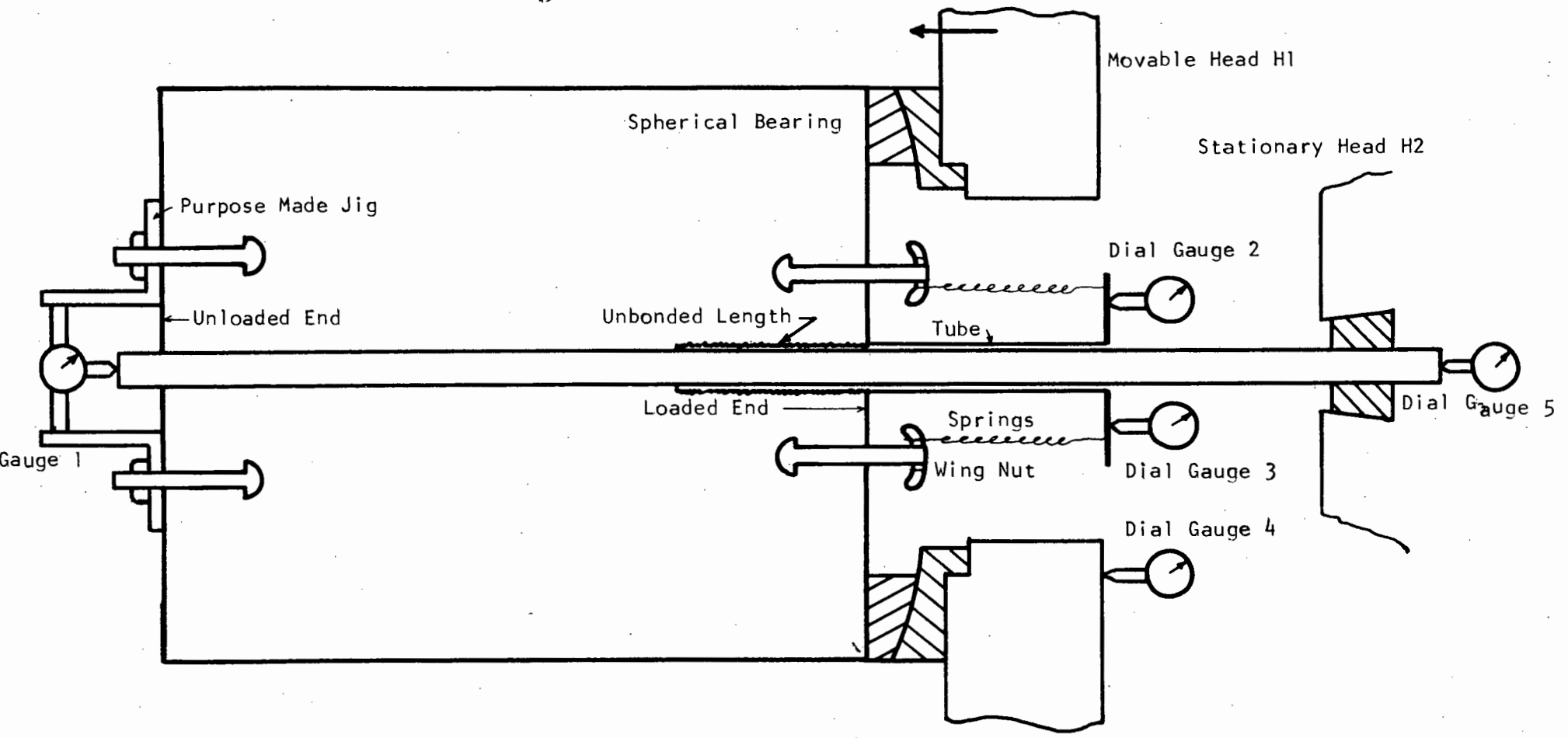

Figure 27 : Position Of Dial Gauges

The heating of the test specimens commenced the day prior to testing - specimens being heated for a total time of 32 hours. The temperature during this time was controlled by a temperature controller in series with an energy controller. (The control of power was necessary to eliminate the large differential temperatures which would be experienced during the initial stages of heating without such control.)

Whilst setting up the specimen in the testing machine and during the testing period (approximately 15 minutes) the heating jackets were turned off.

The distribution of temperature in the test specimens was determined at regular intervals during the testing programme. Copper - constantan thermocouples, cast in the specimens, were used in conjunction with a thermo-multimeter to obtain temperature readings. The temperature curves shown in Figure 28 are obtained from the results presented in Appendix 2.7. The curves are drawn from temperature determinations at the circumference of the specimen and next to the reinforcing bar. From these curves it can be seen that at the higher test temperatures i.e. 350°C, differential temperatures of 40°C were experienced in the radial direction during heating. Furthermore, the temperature at the concrete steel interface did not attain the test temperature - at the 350°C test temperature, the temperature at the interface was approximately 338°C. In the longitudinal direction, maximum differential temperatures of approximately 8°C are found at the 350°C temperature level.

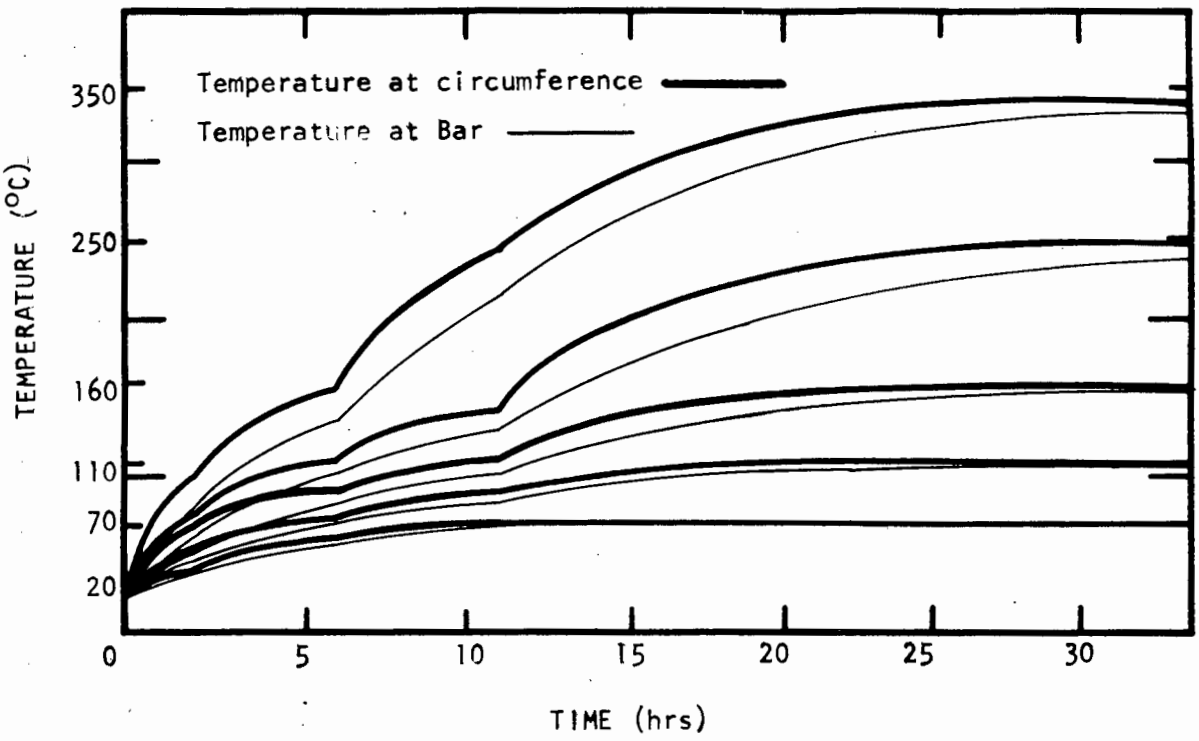

Figure 28 Temperature Versus Heating Time Curves

CHAPTER 4 EXPERIMENTAL RESULTS.

4.1) Presentation Of Results.

The tables shown in Appendix 3.1 give the results of Compacting Factor and cube compressive strength tests (discussed in Chapter 3), together with the ultimate failure load (kN)* and type of failure associated with each bond test. It should be noted that only one batch of concrete was mixed per day. Thus specimens tested on a particular day are grouped together.

The load-slip results, presented in Appendix 3.2 and 3.3 are the average of three load-slip determinations for each type of specimen at each test temperature i.e. the values of slip at a particular load were averaged from three individual tests. It was not possible to present the raw data obtained from the bond tests, due to the bulk of the material.

Results of additional tests for the comparison of the modified and conventional test methods are presented in Appendix 3.4. In this regard, only a limited number of tests were performed, and it is thus possible to give the results of both individual tests, (Tables 3.4.1-9), and the mean obtained therefrom (Tables 3.4.10-14). Modified test results are those determined in the main testing programme.

4.2) Results Of Conventional Pullout Tests.

The conventional pullout test results are compared with those obtained from the modified test, and also correlated with those of other authors.

*All measurements of applied load were in f.p.s. units and have been converted to SI units throughout this thesis.

The mix used for the conventional pullout test was mix M1. The mean compressive strength and Compacting Factor, obtained from the results presented in Table 3.4.10 for this mix, are 57,5 N/mm^2 and 0,921 respectively. These values are not significantly different from the mean compressive strength, 57,5 N/mm^2, and Compacting Factor, 0,916, determined from the main testing programme. The test temperatures were 20°C, 70°C, 160°C, and 350°C, and only 25 mm diameter plain and deformed bars were used for comparison of the two methods of pullout test.

The two types of test are compared with reference to

(i) Bond strength
(ii) Average bond stress versus slip curves.

(i) The mean bond strengths of deformed bar specimens tested at 20°C are 19,6 N/mm^2 and 19,2 N/mm^2 for the conventional and modified tests respectively. Similar values for plain bar specimens are 5,2 N/mm^2 and 5,4 N/mm^2 respectively. It is thus concluded that bond strength at this temperature is independent of the method of test. Residual bond strengths for the two types of test are shown in Table IV. In order to minimize the effects of variations between batches of specimens cast each day, the residuals have been calculated with reference to the 20°C test associated with the particular batch of specimens. Thus three residual determinations are obtained for each temperature and specimen type and the mean of the three residual bond strengths determined. It was not possible to calculate the residual bond strengths in certain cases, because of incompatibility of failure patterns e.g. splitting failure of high temperature specimen and slip failure of reference specimen or vice versa. The mean residuals obtained from Table IV are plotted in Figure 1*. It is apparent from this figure that the

*All figures referred to in this Chapter are found in Appendix A under separate cover. (vide Volume 2).

modified pullout test exhibits greater deterioration of bond strength at high temperatures than the conventional pullout test for both plain and deformed bars. It is interesting to note that the largest difference in deterioration between the two types of test occurs at 160°C. It will be shown in section 4.3 that there is recovery of compressive strength and, to a lesser extent, tensile strength of concrete at these temperatures. The above observation of the difference in deterioration at 160°C thus suggests that the modified test is influenced to a greater extent by tensile strength of concrete than by compressive strength.

The bond strengths obtained in the present investigation are higher than those determined by other investigators. Pullout tests by Mathey and Watstein [21] using 25 mm diameter deformed bars and concrete of 29.2 N/mm^2 compressive strength, produced bond strengths of 8,2 N/mm^2. Untrauer and Henry [24] performed similar pullout tests but used a 150 mm bond length and concrete of 37,2 N/mm compressive strength. They report bond strengths of 12,0 N/mm^2 which was increased to 20,5 N/mm^2 by the application of normal pressure to two parallel faces of the bond specimen. The high bond strengths of deformed bar specimens determined in the present investigation are due to the large size of the specimens tested and the high compressive strengths of the concrete. It should be noted that failure of the specimens with 25 mm deformed bars was accompanied by longitudinal bursting of the concrete into two or three portions. Thus the bond strengths of these specimens is not a true bond strength but a measure of the tensile strength of the concrete. In the present investigation, cylindrical specimens 305 mm long were used, as compared with those of Watstein which had a length of 200 mm. The bond strengths of plain bars reported by Clark [14] are 4,2 N/mm^2. Clark used 22 mm diameter plain bars and concrete of compressive strength

38,6 N/mm^2. The present investigation produced bond strength of 5,4 N/mm^2 for plain bars. Reloading of plain bars after failure reduced the bond strength by as much as 35%. This indicates that the adhesion and, in particular, the mechanical interlocking of rugosities and concrete, of the plain bars was substantial.

TABLE IV - RESIDUAL BOND STRENGTHS
CONVENTIONAL PULLOUT TEST.

	DEFORMED BAR				PLAIN BAR		
	20°C	70°C	160°C	350°C	70°C	160°C	350°C
	100	95	93	92	82	76	60
	100	97	94	87	84	79	67
	100	95	92	70	85	70	71
Av:	100	96	93	84	84	75	66

MODIFIED PULLOUT TEST.

	DEFORMED BAR				PLAIN BAR		
	20°C	70°C	160°C	350°C	70°C	160°C	350°C
	100	- *	86	89	88	76	61
	100	89	92	82	85	54	59
	100	96	96	83	68	72	71
Av:	100	93	91	85	80	67	65

* Failure by slipping.

(ii) Average Bond Stress.

The average bond stress versus slip curves of the conventional pullout test and the modified test methods shall be compared in two sections.

(a) Unloaded - end slip
(b) Loaded - end slip.

(a) Unloaded - End Slip.

The unloaded-end slip curves for plain bars at temperatures of 20°C, 70°C, 160°C and 350°C are shown in Figure 2. It is apparent from the curves in this figure that at a particular bond stress, greater values of slip are obtained in the conventional tests than in the modified tests at all temperatures.

A similar conclusion may be deduced from the unloaded-end slip curves of deformed bars presented in Figure 3. However, the slip produced in the conventional test at 20°C does not differ significantly from that produced in the modified test. At the higher temperatures the difference between the two types of test is more pronounced.

In Table V, the residual average bond stress at 0,010 mm slip for deformed and plain bar specimens is presented. These values were determined by interpolation of the mean bond slip Tables 3.4.11-12. From Table V, greater deterioration of bond in the conventional than in the modified tests on deformed bar specimens is apparent. However,no significant difference in deterioration of bond between the two types of test using plain bars is indicated.

(b) Loaded - End Slip.

The loaded-end slip curves are shown in Figures 4 and 5. From these curves similar trends to the unloaded-end slip curves may be observed. However, the difference in slip between the two types of test at a particular bond stress,

is more marked in the loaded-end slip results than the unloaded-end slip. This is due to two factors:

(a) the displacement and deformation of the loaded-end concrete face,
(b) the pinching effect of the normal compressive stresses near the unloaded-end of the modified pullout test.

TABLE V - RESIDUAL AVERAGE BOND STRESS AT 0,010 mm SLIP.

SPECIMEN	CONVENTIONAL TEST				MODIFIED TEST			
	20°C	70°C	160°C	350°C	20°C	70°C	160°C	350°C
M1/D/25	100	69	73	20	100	80	93	35
M1/P/25	100	77	54	23	100	80	53	25

The effect of the deformation of the loaded-end concrete face on the readings taken there, can be explained with reference to Figure 6. Points P_c and P'_c are the original and final positions respectively of the concrete surface due to the application of a load F to the bar. In the case of the modified test, it can be seen that the deformation of the concrete decreases the amount of slip produced i.e. the concrete surface displaces $\Delta H - \Delta C$ in the modified test but displaces ΔH in the conventional test.

where ΔH = displacement of bearing plate
ΔC = deformation of concrete surface.

A comparison of the authors unloaded-end slip results with those of Clark [14] and Ferguson [8] is made in Figure 7. The conventional test method used in this investigation produced results of unloaded-end slip which are in good agreement with those of Clark and Ferguson. It should be noted that 22 mm diameter bars were used in both Clark and Ferguson's tests. Furthermore, concrete of 27 N/mm^2 compressive strength was used by these investigators. This would account for the slightly lower values of slip obtained by Clark in his tests with plain bars. The lower values of bond stress at high slip observed by Clark and Ferguson in their deformed bar specimens, may also be attributed to the weaker concrete compressive strength used by these authors.

Conclusions.

In general, the results indicated that greater slips are produced in the conventional than in the modified test.

The tests also established that the modified and conventional test methods produce similar bond strengths at room temperature only. Significant differences are observed at higher temperatures.

The results of the conventional test agree with those of other authors, although larger bond strengths were observed in the present investigation.

The significance of the loaded-end concrete displacement will be fully covered in Chapter 5.

4.3) Bond Strength Results Of Modified Pullout Tests.

Two distinct types of bond strength failure were observed in these tests:

(a) Bond strength obtained by bursting of specimens - predominant in the tests on 25 mm deformed bars.

(b) Bond strength obtained by slipping of the reinforcing bar - predominant in the test on plain bars and 12 mm deformed bars.

Similar failure patterns have been observed by other investigators [7], [8], [14] using high-bond deformed bars. A third type of failure, viz. tensile failure of the steel, was not considered in the determination of bond strength. Tensile failure of the steel only occurred in 12 mm diameter deformed bar specimens.

The mean bond strengths at test temperature of 20°C for a particular specimen have been summarized in Table VI.

TABLE VI.

Mean Bond Strength at 20°C (N/mm^2)

Bar \ Mix	M_1	M_2	M_3	M_4
D/25	19,42	19,91	15,96	16,22
D/12	11,47	11,23	10,76	10,51
P/25	5,53	5,34	4,91	5,00
P/12	5,50	5,26	4,59	4,67

It is apparent from the values in Table VI that the bond strengths of the high strength mixes, M1 and M2, are significantly greater than those of the low strength mixes, M3 and M4. In this respect, an increase in compressive strength of 54% has produced an increase in bond strength of 23% and 7% for specimens which failed by bursting and slipping respectively.

Residual bond strengths for all tests performed at elevated

temperature are presented in Tables 3.5.1-4. The mean residuals calculated from these results are plotted in Figures 8-11. From these graphs the following trends are noticeable:

(a) In general, increase in temperature is accompanied by decrease in bond strength.
(b) Greatest deterioration of bond strength occurs at 100°C for deformed bar specimens - between 12% and 25%.
(c) Partial recovery of bond strength is exhibited between 160°C and 250°C for specimens M1/D/25 and M1/D/12. However, no recovery in bond strength at these temperatures is apparent for plain bar specimens.
(d) Elevated temperatures produce greater deterioration of bond strength of plain bar specimens than of deformed bar specimens.
(e) The mixes of high water/cement ratio exhibit greater bond strength deterioration than those of low water/cement ratio.

Discussion of Bond Strength Results.

The review of literature [7] [8] has shown the dependency of bond strength on the strength of conrete. Variations in concrete strength (both flexural and compressive) with temperature could thus be expected to produce similar variations in bond strength. Numerous investigators [25], [29], [30], [31] have shown that concrete physical properties decrease in magnitude with increase in temperature. Reductions in compressive strength of up to 30% occur at temperatures of 100°C. This reduction in strength is attributed to the partial removal of evaporable water. Disruptive strains between gel particles are produced by the remaining, expanded load bearing water. At temperatures above 100°C, a more complete removal of water results in gel crystallites moving closer together and in places solid-solid bonding can develop. An increase

in cement paste strength is produced and complete or partial recovery of compressive strength is observed. Microcracking of the hydrated cement paste and fracture of the bond between paste and aggregate are responsible for a resumption of compressive strength loss above 300°C. No further recovery is observed at higher temperatures. Flexural strength [29],[30],[31] was found to follow a similar pattern of deterioration to that indicated by compressive strength. Reductions in flexural strength are greater than those incurred in compression - 50% reduction at 100°C and only partial recovery at 200°C. The bond strength of deformed bar specimens tested in this investigation have shown similar fluctuations of deterioration with temperature as the compressive and flexural strength of concrete. The greater decrease in tensile strength of the concrete than its compressive strength explains the more pronounced deterioration of bond strength in 25 mm deformed bar specimens than of 12 mm deformed bar specimens. Although slight increases at 350°C were obtained this was not considered significant. The bond strength of plain bars decreases rapidly with increase in temperature. In this regard, the effect of temperature on the adhesion and friction of the bar is significant. Differential expansion of the bar and concrete in the longitudinal direction at high temperatures causes disruptive strains at the interface and the consequent breakdown of bond.

4.4) Unloaded End Slip Results Of Modified Pullout Tests.

The effects of temperature on unloaded end slip will be considered in two sections.

(i) Trends observed in the unloaded end slip versus average bond stress curves.

(ii) The effect of temperature, bar diameter and concrete properties on the average bond stress at 0,01 mm slip.

(i) The average bond stress versus unloaded end slip curves illustrated in Figures 12-27 are plotted from the values presented in Tables 3.2.1-16. The following effects of temperature on slip resistance are apparent from these curves:

(a) Slip resistance decreases with increase in temperature for all types of bar.
(b) Greatest deterioration in slip resistance for deformed bar specimens occurs at 110°C - this is not found in the results for plain reinforcing bars.
(c) At 350°C, there is a partial recovery of slip resistance for deformed bars at high average bond stress.

(ii) The values of average bond stress at 0,01 mm slip shown in Tables 3.6.1-6 were determined by Aitkens method of interpolation using a package programme on an I.B.M. 360 computer. Mean residual average bond stresses were calculated as explained in section 4.2 and are plotted in Figures 28-31.

The effect of temperature on the deterioration of slip resistance at 0,01 mm slip for both deformed and plain bars is apparent from these Figures. Each type of bar will be considered separately.

(a) Deformed Bars.

It is apparent from Figures 28 and 29 that at 70°C the deterioration of slip resistance for D/25 bar specimens is between 20% - 30% and up to 30% for D/12 bar specimens. The gain in slip resistance of M1/D/12 specimens at 70°C over those at room temperature, is not considered significant - this gain is not exhibited by other specimen types. Small recovery of slip resistance is manifest at 160°C for certain deformed bars, viz. M1/25, M2/25, M4/25, M3/12 and M4/12. In general, the effect of temperature,

per se, on the bond is greater than that of variations in concrete compressive and flexural strength as mentioned in Section 4.3. At 350°C the bond deteriorates to between 40% - 86% for 25 mm deformed bars and 56% - 70% for 12 mm deformed bars.

(b) From Figures 30-31 the deterioration of bond with increase in temperature is again apparent. At 350°C the average bond stress of P/25 bar specimens is only between 25% - 40% of the reference temperature average bond stress. The average bond stress of P/12 bar specimens at the same temperature, is between 37% and 53% of its original value. In general, greater loss of bond is exhibited by P/25 specimens than P/12 bar specimens at all temperatures.

It is difficult to isolate the effects of the test parameters i.e. bar diameter and concrete properties, on the deterioration of bond. To overcome this difficulty, recourse is made to a statistical analysis of the interpolated values of average bond stress at 0,010 mm slip.

Analysis of variance was performed on:

(a) Average bond stress values at 0,010 mm slip
(b) Differences of average bond stress values at test temperature from those at room temperature.

(a) A two way analysis of variance was performed on the average bond stress values at 0,010 mm slip using a package programme on an I.B.M. 360 computer. The A and B treatments of the analysis were bar diameters and concrete mixes respectively. Computerized results are given in Appendix 3.7 and these are summarized in Tables VII and VIII.

TABLE VII - Analysis Of Variance Of Average Bond Stress For Plain Bars.

Probability For Acceptance Of Null Hypothesis.

Temp	20°C	70°C	110°C	160°C	250°C	350°C
A	0,0000	0,0000	0,0000	0,0006	0,0000	0,0004
B	0,0003	0,0018	0,0695	0,5013	0,0832	0,4314

TABLE VIII - Analysis Of Variance Of Average Bond Stress For Deformed Bars.

Probability For Acceptance Of Null Hypothesis.

Temp	20°C	70°C	110°C	160°C	250°C	350°C
A	0,0000	0,0000	0,0000	0,0038	0,0000	0,0000
B	0,0210	0,0002	0,0013	0,8566	0,8620	0,0050

The Null hypothesis of the bar diameter or the concrete mixes affecting the results of the average bond stress is rejected at the 5% level of significance. From the tables it can be seen that the bar diameter influences results at all temperatures. This is to be expected, as the constant bond length used in this investigation and in the determination of the bond stresses, leads to a smaller bond area (and, therefore, a greater bond stress) being used in the calculations on 12 mm bars than

on 25 mm bars. The concrete mixes appear to be significant in influencing the values of average bond stress at low temperature levels only, i.e. up to temperatures of 70°C for plain bars and 110°C for deformed bars. However, the above analysis does not reflect the individual contributions of concrete compressive strength and workability on the slip resistance at various temperatures.

A similar analysis with 'A' and 'B' treatments of concrete strength and workability respectively, produced the results shown in Table IX. The results are not as reproducible as in the previous analysis, but two facts are established. Firstly, compressive strength affects the slip of both types of bars at low temperature and, secondly, workability influences plain bar slip at 20°C.

TABLE IX - Analysis Of Variance Of Average Bond Stress At 0,01 mm Slip With Concrete Compressive Strength And Workability As Test Treatments.

Probability For Acceptance Of Null Hypothesis.

Temp	20°C	70°C	110°C	160°C	250°C	350°C
Bar: D/25						
A	0,0425	0,005	0,5172	0,5594	0,8159	0,0861
B	0,1866	0,087	0,1952	0,8973	0,5219	0,1721
Bar: D/12						
A	0,0351	0,0033	0,008	0,7582	0,2720	0,0056
B	0,2212	0,0251	0,36711	0,3313	0,1185	0,5067

TABLE IX (Contd.)

Temp	20°C	70°C	110°C	160°C	250°C	350°C
Bar: P/25						
A	0,6479	0,0222	0,8514	0,0561	0,3620	0,8249
B	0,0051	0,2150	0,6417	0,1592	0,0327	0,2191
Bar: P/12						
A	0,0072	0,6469	0,1728	0,8670	0,0668	0,2260
B	0,0324	0,0696	0,1229	0,7498	0,8078	0,8774

(b) The results of a two way analysis of variance on the deterioration of average bond stress at 0,010 mm slip, are shown in Tables X and XI. The 'A' and 'B' treatments of the analysis are bar diameter and concrete mixes respectively. The analysis was performed to indicate the effect exerted by bar diameter and concrete properties on the deterioration of bond.

TABLE X - Analysis Of Variance Of Deterioration Of Average Bond Stress For Plain Bars.

Probability For Acceptance Of Null Hypothesis.

Temp	70°C	110°C	160°C	250°C	350°C
A	0,0020	0,0430	0,6544	0,2385	0,5893
B	0,0037	0,0378	0,4068	0,9751	0,0122

TABLE XI - Analysis Of Variance Of Deterioration Of Average Bond Stress For Deformed Bars.

Probability For Acceptance Of Null Hypothesis.

Temp	70°C	110°C	160°C	250°C	350°C
A	0,9843	0,4911	0,2435	0,4860	0,5011
B	0,0200	0,0844	0,7389	0,3552	0,1419

It is apparent from Tables X and XI that rejection of the null hypothesis at the 5% level of significance indicates dependency of bond deterioration on the concrete properties at low temperatures.

The bar diameter effects the deterioration of bond of plain bars at 70°C and 110°C only. The deterioration of bond for deformed bar specimens is independent of bar diameter, i.e. both 25 mm and 12 mm diameter deformed bars exhibit similar deterioration.

Discussion Of Unloaded End Slip Results.

The results of the present investigation on bond do not compare favourably with those published by Harada et al[20]. The present investigation shows deterioration of bond at 110°C for 12 mm deformed bars to 60% of original bond at room temperature. Harada indicates residuals of 45% at 100°C for 13 mm diameter deformed bars and 0,050 mm slip. It should be noted that Harada performed his tests after cooling the specimens to room temperature. This gradual cooling process would further disrupt the bond due to contraction of the steel. Their [20] investigation shows residuals which agree with those of present investigation at temperature of 300°C i.e. 45%.

The effect of temperature on the bond between concrete and steel appears to be dependent upon:

(a) Temperature level,
(b) Deterioration of concrete properties with increase in temperature,
(c) Type of bar,
(d) Level of average bond stress.

(a) Temperature Level.

The temperature has been shown to breakdown the bond between concrete and steel and to produce deterioration in concrete strength. (The dependence of bond on concrete strength will be discussed separately).

In section 4.3, the detrimental effect of temperature on the adhesion and friction bond was discussed. Thus temperature, per se, causes greater deterioration on the bond of plain bars than of deformed bars. The influence of temperature on plain bar bond is clearly defined in the analysis of variance performed on the average bond stress values at 0,010 mm slip. It is concluded that breakdown of bond at temperatures higher than 110^{o}C is large enough to override any additional influence of concrete properties. The greater disruption of bond due to temperature in the case of 25 mm diameter plain bar specimens than of 12 mm diameter plain bar specimens will be discussed later. (vide type of bar). The bond of deformed bars is only effected by temperature at small values of slip i.e. during the adhesion and friction stages of bond. This aspect of temperature influence was not determined.

(b) Deterioration of Concrete Properties with Increase in Temperature.

Slipping of deformed bars has been shown in the literature [2], [5] to be influenced by the geometry of the rib. In this respect, the rib face angle was of great importance.

Due to the variability of this property in the steel used, it was not possible to determine the rib face angle accurately - an estimate of between 40^{o} and 60^{o} was made. Slipping of the bars, particularly at high levels of bond stress, was accompanied by crushing of the concrete at the rib interface. This was substantiated by observations of the concrete key between ribs of deformed bars pulled out of the concrete matrix. For 12 mm diameter deformed bars, the concrete key occupied the whole distance between the ribs. Only part of this key (5mm) was developed in the case of 25 mm deformed bars which failed by slipping. Bars which had burst the specimens showed that considerable compaction and slip had taken place at the ribs. Similar results are presented by Lutz [2] and Rehm [5]. The $\frac{c}{h}$ ratios for the deformed bars used in the present investigation are 12 and 7 for 25 mm and 12 mm diameter bars respectively. Rehm's estimate of $\frac{c}{h}$ less than 7 for the concrete key to occupy the full distance between the ribs, is thus confirmed. The slip of deformed bars is dependent upon the compressive strength of the concrete. The above observations of the slip of deformed bars used in this investigation substantiates this fact. The slip resistance has been found to follow similar deterioration patterns to those of concrete compressive strength with increase in temperature. The low slip resistance at $110^{o}C$ in the case of deformed bars is of particular significance, as it corresponds with the greatest deterioration of concrete strength with increase in temperature. There is recovery of slip resistance at temperatures above $110^{o}C$, with the largest increases at $160^{o}C$ and gradual deterioration at higher temperatures. The analysis of variance of average bond stress at $160^{o}C$ and $250^{o}C$ indicates that the concrete properties exerted no influence on the bond at these temperatures. This suggests that the recovery of concrete strength is such as to effectively eliminate the differences in magnitude of concrete compressive strength and thus minimizes the effect of this parameter on the variance of average bond stress.

(c) Type of Bar.

The results of the bond tests have shown that both bar diameter and deformation pattern i.e. plain or deformed, substantially influence the slip resistance.

Deformed bars.

The analysis of variance performed on the average bond stress values of deformed bars at 0,010 mm slip, show large dependency of these results on the bar diameter. Various authors [2], [14] have compared bars of different diameter but with similar $\frac{\text{diameter (D)}}{\text{length of embedment (L)}}$ ratios. The ratio of $\frac{D}{L}$ for the 25 mm and 12 mm diameter bars used in the present investigation is 0,1250 and 0,0600 respectively. Thus, at a particular slip, the 12 mm diameter bar is expected to develop twice the average bond stress of the 25 mm diameter bar. In the present series of tests, the 12 mm bar developed 1,3 times the average bond stress of 25 mm bars at the 0,010 mm value of slip. It is concluded that the analysis of variance would have produced similar results to that performed in section 4.3 if the 12 mm bar average bond stress values had been corrected for $\frac{D}{L}$ ratio i.e. if the average bond stress for 12 mm specimens was decreased by a factor of 2. From the residual average bond stress versus temperature curves, no significant difference in deterioration of bond is apparent with different diameter bars. Although bar diameter effects the value of bond stress at a particular slip i.e. smaller bar diameter exhibits larger bond stresses, temperature change has no influence on the effects that bar diameter has on the slip resistance of deformed bars.

Plain Bars.

The bond of plain bars is shown in the literature review to be predominantly an adhesion and friction effect. In this regard, shrinkage of the concrete which is dependent primarily on the quantity of water per unit volume [37], is important in bond development. This is substantiated by the analysis of variance which indicates that workability

affects slip resistance at low temperatures. The fact that 12 mm diameter bars exhibit less deterioration of bond with increase in temperature than 25 mm diameter bars is to be expected. Rugosities on the surface of the bar would affect the bond of 12 mm diameter bars to a greater extent than that of 25 mm diameter bars.

(d) Level of Average Bond Stress.

Results of the tests on deformed bars showed that the level of average bond stress is an important factor in these tests. The collection of water and air bubbles below the ribs of the bars during casting of specimens in this investigation and their influence on the test results is difficult to assess. Removal of evaporable water from the concrete matrix at 100^{o}C and the consequent creation of voids at the rib interface would account for the large deterioration of slip resistance at all levels of bond stress. However, at high levels of average bond stress, considerable compaction takes place at the concrete steel rib interface (vide section 4.3 section c) and the concrete compressive strength would be the controlling parameter for slip.

4.5) Loaded End Slip Results Of Modified Pullout Test.

The average bond stress versus loaded end slip curves for all specimens at different temperatures are illustrated in Figures 32 - 47. These curves were plotted from the results presented in Tables 3.5.1-16.

No correction has been applied to these slip values for the extension of the reinforcing bar between the loaded end concrete surface and the stationary head H2 of the testing machine. The variation in the Young's Modulus of steel due to temperatures up to 350^{o}C is negligible[39] (less than 3%) and the same correction would have been applied to similar diameter bars. (It should be noted that

no attempt is made to compare the unloaded end slip results of different diameter bars.)

The loaded end slip curves for deformed bars illustrated in Figure 32 - 39 indicate the following similar trends to those established from the unloaded end slip curves, viz.:

(a) Increases in temperature decrease slip resistance.
(b) Greatest deterioration of slip resistance occurs at 110°C.
(c) Recovery of slip resistance is manifest at 350°C after considerable slip has taken place.

However, the loaded end slip results contradict trend (a) at 70°C i.e. increased slip resistance over that at 20°C is found at this temperature. The results of loaded end slip have been shown in section 4.3 to be influenced by the deformation of the loaded end concrete surface. It was indicated that values of the loaded end slip were decreased by deformation of the concrete. The author suggests that at 70°C the deterioration of concrete properties i.e. Young's Modulus and tensile strength, would cause larger deformation to occur and thus, less noticeable slip. The effect of temperature on the bond, per se, at temperatures above 70°C is more important than that due to concrete deformation indicated above. Consequently, slip resistance is decreased at these temperatures.

In Figures 40-47, the average bond stress versus slip curves for plain bar specimens are shown. From these figures, it can be seen that the deterioration of slip resistance at high temperatures for loaded end follows similar trends as the unloaded end slip. The 70°C temperature increase in slip resistance discussed above, is also manifest in the plain bar specimen results.

4.6) Conclusions.

(i) Bond Strength.

The present investigation has shown the marked deterioration of bond strength with temperature of all types of bar and different mixes. In addition it has been noticed that with respect to bond strength:

(a) For deformed bars the greatest decrease occurs at 110°C. This has been attributed to deterioration in concrete strength at this temperature.

(b) Recovery of bond strength is exhibited between 160°C and 250°C for deformed bar specimens. Again this is attributed to recovery of concrete strength at these temperatures as reported by various investigators. Plain bars do not exhibit any recovery of bond strength at 160°C or 250°C.

(c) Greater deterioration of bond strength at elevated temperatures is shown in the results for plain bar specimens than in those for deformed bar specimens. This is due to the direct influence of temperature on the bond of plain bars.

(d) Mixes of high w/c ratio exhibited greater bond strength deterioration than those of low w/c ratios. In general, the large effect of temperature made it difficult to isolate the influence of concrete properties on bond strength.

(ii) Unloaded End Slip.

The temperature level has shown a large influence on the slip resistance of all types of bar. This influence is manifest both directly by breakdown of bond due to differential expansion of concrete and steel, and also

indirectly through the effects of temperature on the strength of concrete. With reference to the unloaded end slip, the investigation established that:

(a) Increase in temperature results in decreases of slip resistance for all types of bars tested.

(b) The largest decrease in slip resistance for deformed bars was manifest at 110°C. At higher temperatures recovery of slip resistance was exhibited by deformed bars but not in the case of plain bars.

(c) The residual average bond stress at 70°C decreased to 70% for 25 mm and 12 mm deformed bar specimens. Loss of bond resulted in residuals of between 70% and 95% for the average bond stress of plain bars.

(d) Greater loss of bond was exhibited by 25 mm plain bars than 12 mm plain bars at all temperatures. The residuals of average bond stress at 350°C were between 25% - 40% and 37% - 53% for plain 25 mm and 12 mm diameter bars respectively.

(e) Mix proportions affect plain and deformed bar specimens average bond stress at temperatures below 110°C. In particular, concrete strength was shown to affect the bond of both deformed and plain bars and workability that of plain bars only.

(f) Bar diameter affects the magnitude of average bond stress at a particular slip, but does not influence the deterioration of the bond with increase in temperature.

(iii) Loaded End Slip.

The deterioration of average bond stress with temperature shown by the loaded end slip curves followed similar trends to those indicated by the unloaded end slip curves. In

particular it was established that:

(a) Less slip occurs at 70°C than at 20°C for all types of bar.

(b) The greatest deterioration of slip occurred at a temperature of 110°C.

(c) At temperatures above 110°C the slip resistance decreased with increase in temperature.

(d) At 350°C, some recovery of slip resistance was observed at high slip values.

The method of pullout testing employed in this investigation produced results which conclusively indicated that deformation and cracking of the concrete at the loaded end influenced the slip produced at this concrete surface. Under load application, decrease of concrete strength with temperature caused large deformation of the unloaded end concrete surface, and at 70°C this deformation was large enough to override the effects of temperature on the bond and consequently, smaller slip at a particular average bond stress was measured at 70°C than at the reference room temperature.

A theoretical analysis of the stress patterns in pullout tests follows.

CHAPTER 5 - AXISYMMETRIC FINITE ELEMENT ANALYSIS OF BOND SPECIMEN.

5.1) INTRODUCTION.

The use of a modified pullout test in the present investigation on bond, requires a knowledge of the stress distribution and concrete displacements within the bond specimen during the application of load. This knowledge of stresses and displacements is essential if an evaluation of the test method is to be made.

The greatest problem encountered in a finite element analysis of reinforced concrete structures is the simulation of the load-slip characteristics of the bond between the reinforcing bars and concrete. The problem is complicated by the non-linear stress strain relationship for concrete and the cracking of the concrete under increasing load. Furthermore, the literature review (vide Chapter 2) has indicated the dependence of bond on bar geometry and concrete properties. It is not the intention of the present analysis to solve the problem of bond simulation but to provide a solution to the analysis of stress for the case of a bar embedded in concrete and to determine the influence of slip, at low loads, on the stresses.

5.2) REVIEW OF LITERATURE.

The stresses and deformations produced by loading of reinforcing bar embedded in concrete have been theoretically examined by various authors [5], [34], [36]. The results obtained have often been unsatisfactory, as simplifying assumptions such as uniform concrete stresses, no consideration for the effects of cracks, perfect bond, are normally made.

Rehm's [5] theoretical treatment of bond stress has been presented in Chapter 2. This analysis assumes different load-slip relationships at various values of bond stress.

Thus at low loads a linear relationship is postulated, whereas at higher loads, when slip involves mechanical interlocking of ribs and concrete matrix, the relationship assumes slip to be raised to a power less than one.

Broms [34] analysed the concrete stresses produced between two cracks near a reinforcing bar. His two dimensional analysis of a three dimensional problem is considered to be qualitative at best, but it does indicate that high longitudinal and transverse tensile stresses occur in the concrete at the level of the reinforcement.

Lutz [36] used an axisymmetric finite element method to solve for the stresses produced by a steel bar embedded in a cylinder of concrete. He examined two models with different boundary conditions, viz.:

(a) Reinforcing bar loaded at both ends to simulate conditions between flexural cracks. The cracks were assumed to be 6 x D apart

where D = diameter of bar.

(b) Reinforcing bar loaded at one end and the reaction provided by shear forces on the outer cylindrical surface to simulate conditions in the anchorage zone of a beam.

The flexural zone stresses were examined by assuming steel-concrete interface conditions of perfect bond, limited length (1,5 x D) of separation and slip between the steel and concrete, and slip over 2,5 x D of length of specimen from the loaded end. The perfect bond case indicates extremely high radial stresses at the intersection of the steel-concrete interface with a transverse crack. Radial separation at the transverse crack is thus expected. This separation is simulated in the second analysis with slip occurring over 1,5 x diameter of bar from the transverse crack.

The longitudinal stresses in the concrete at the steel were found to be large enough to indicate that additional transverse cracks would form at the surface of the reinforcing bar. These cracks would be reduced or prevented if sufficient slip occurred to reduce the longitudinal stress below the cracking stress. The final analysis established that bond stresses and radial separation decrease in magnitude, although the tensile longitudinal stress in the concrete is still large enough to indicate additional cracking must occur.

The anchorage zone stresses were determined by an elastic analysis of a concrete cylinder (152 mm diameter and 381 mm long) with a 25,4 mm diameter reinforcing bar embedded along the axis of the cylinder. Three analyses were made. In the first, separation was allowed to occur for 6,35 mm from the loaded end with perfect bond over the rest of the specimen length. This analysis indicated that large tensile radial stresses occur at the loaded end. Tensile longitudinal and circumferential stresses in this region were also extremely large. In the second analysis, separation was allowed to occur for 63,5 mm from the loaded end.

Longitudinal and shear stresses were reduced by up to 30% of those obtained for 6,35 mm separation. The increased separation reduced the radial tensile stresses but increased the circumferential stresses by 20%. The final analysis considered slip and separation to be dependent upon a bond-slip relationship which was determined experimentally by Lutz. The longitudinal, circumferential and shear stresses were almost one-half those found in the previous solution. Lutz concluded that the stresses produced near a transverse crack in the anchorage zone are similar to those found in the flexural zone. Both analyses indicate the large probability of additional transverse and splitting cracks occurring.

5.3) ANALYSIS OF BOND SPECIMEN.

The cylindrical bond specimen used in the experimental section of this thesis requires a three dimensional elas-

tic solution for its analysis. Since the load transfer from the steel to concrete is axisymmetric, an axisymmetrical solution was decided upon.

The formulation of the general axisymmetrical finite element procedure is based on Zienkiewitz [18]. A listing of the programme is given in Appendix 4.1.

A ring element with a triangular cross section is used in the analysis. This allows the cross sectional area of the rings to be varied easily, which could not be done with a rectangular shape. Subdivision of the cylindrical specimen into triangular ring elements is shown diagrammatically in Figure 48*. Three hundred and forty eight elements are used. The Young's Modulus and Poisson's Ratio of the concrete and steel are assumed to be 30 GPa; 0,15 and 200 GPa; 0,30 respectively.

The load vector consists of a single load of 4480 N applied to the circumference of the 25 mm diameter reinforcing bar at the loaded end concrete surface. The load is the smallest value at which loaded end slip was observed in the experimental section of the present investigation.

Boundary conditions applied are zero longitudinal displacement of the concrete at the loaded end bearing surface. Frictional resistance restrains the displacement of the concrete at the bearing surface in a radial direction. An analysis with no radial concrete displacement at the bearing nodes indicated that the stress distribution at the interface was not significantly affected by this restriction.

* All figures referred to in this Chapter are found in Appendix B under separate cover.

(i) Results of Assumed Perfect Bond Analysis.

Results of Lutz analysis of a bar embedded in concrete to simulate anchorage zone stresses are indicated in Figure 49. A similar model was analysed using the programme developed for the present finite element investigation. Results of this analysis are also shown in Figure 49 for comparison with those obtained by Lutz. The longitudinal and bond shear stresses at the bar-concrete interface agree closely for the two analyses except near the loaded end. Lutz assumed separation and slip for 6,35 mm from the loaded end which would account for the decrease in stress magnitude at this point. The radial stresses are particularly affected by this boundary condition. In general, the results produced are not significantly different from each other in magnitude and distribution.

(a) Stress at Interface for Modified and Conventional Test Methods.

The results of the stress analyses of the modified and conventional test specimens are shown in Figures 50 and 51. A comparison of the two diagrams establishes that with respect to stress magnitude, larger compressive longitudinal stresses are produced at the loaded end in the conventional test than in the modified test. However, the tensile longitudinal stresses along the bond length are similar in both types of test. Separation of the bar from concrete is inhibited in the modified test method, as concluded from the low value of tensile radial stress produced at the point of load application. In this respect, the tensile radial stresses are twice as large in the conventional test as in the modified test. Near the unloaded end, the radial stresses become compressive in the modified test. This is not considered significant, although at higher loads, this arching effect would be magnified. In both analyses, the maximum circumferential stresses are shown to be only half the maximum longitudinal stresses.

However, the bond shear stresses are large enough to suggest that the adhesion and friction stages of bond are severely disrupted at the point of load application.

(b) Displacement of Concrete at Interface for Modified and Conventional Test Methods.

The radial and longitudinal concrete displacements at the bar-concrete interface for both methods of bond test are illustrated in Figures 51 and 52 respectively. The large radial contraction of the steel bar indicates that slip and separation will occur in the vicinity of the load point, especially as the tensile bond or adhesion between steel and concrete is the weakest mechanism of bond. (vide page 10). At the loaded end, the longitudinal displacement of the concrete in the modified test is 35% of the maximum displacement at the point of load application. Consequently, the loaded end slip of the modified test may be up to 30% less than that of the conventional test under the same load - the maximum longitudinal displacement of both methods of test differ by less than 5%.

(ii) Slip Simulation of Plain Reinforcing Bar Embedded in Cylinder of Concrete.

The effect of slip and separation on the stresses produced in the bond test are considerable [36]. The bond between concrete and steel is simulated in the following analyses by a two dimensional linkage element, introduced at the radial points on the concrete-steel interface. Ngo and Scordelis [35] developed the element for use in the solution of singly reinforced concrete beams on simple supports with different idealized cracking patterns. Their analysis of an uncracked beam using the linkage element to simulate slip, produced results in good agreement with solutions obtained from linear elastic analysis based on transformed section concepts.

The linkage element is diagrammatically illustrated in Figure 54. The element has two nodes, each with two degrees

of freedom. The element stiffness matrix is developed in Appendix 4.2.

Two analyses were performed using the linkage element.

(a) Perfect bond simulated by the linkage element.

(b) Assumed slip and separation by the linkage element.

Loading and boundary conditions were the same as those used for the perfect bond analysis in the previous section. The modified test specimen was analysed throughout.

(a) Perfect Bond Analysis.

Determination of the linkage longitudinal stiffness, A_z, and radial stiffness, A_r, was accomplished by trial and error. The perfect bond analysis required large values for A_z and A_r, and these were arbitrarily chosen as 10^{10} N/mm and 10^{12} N/mm respectively. (Using these values for the linkage stiffness, negligible loaded end slip of 0,0005 mm was determined).

The stresses at the interface determined by the analysis are illustrated in Figure 55 and compared with those obtained in the previous section, shown in Figure 50. In general, good agreement between the two analyses with respect to stress magnitude and distribution is achieved. However, the magnitude of the maximum longitudinal and bond shear stresses are slightly larger in the analysis with linkage elements and small variations in distribution of circumferential stresses are also apparent. Due to the fact that the values of A_z and A_r were arbitrarily assigned, these discrepancies are not significant. Radial displacement of the concrete at the interface is plotted in Figure 52. A comparison with the previous analysis - also shown in Figure 52, indicates that no significant difference between the results is apparent.

(b) Analysis with Assumed Slip.

The determination of the linkage stiffnesses to be used in this analysis presented formidable problems. The longitudinal stiffness was established by increasing its value in all linkages until the loaded end slip was similar to that obtained in the experimental investigation on the bond of plain, 25 mm diameter bars. The value of 250 x 10^3 N/mm thus obtained is smaller than that calculated from the bond test results - approximately 350 x 10^3 N/mm (vide Appendix 4.2). Determining the value of A_r involved an assumption with respect to the radial separation. The perfect bond analysis of the previous section (a) indicated that separation may be expected for a length of 75 mm from the load point. The linkage radial stiffness in this length was decreased to produce separation of 1,2 x 10^{-4} mm and a value of A_r = 5 x 10^5 thus obtained. Although the value of 1,2 x 10^{-4} mm for separation of steel from concrete was arbitarily chosen, it is large enough to ensure breakdown of adhesion bond at the load point. Zero radial separation over the remaining length of interface (125 mm from unloaded end) was assumed and A_r = 10^{12} N/mm assigned to the linkage stiffnesses in this region.

The results of radial concrete displacement determined by this analysis are compared with the perfect bond results in Figure 52. The introduction of the smaller value of A_r mentioned above produces the required separation and also reduces the radial displacements near the loaded end by 15%.

The magnitude and distribution of the concrete stresses along the length of interface are indicated in Figure 56. The following changes in stress from the perfect bond case illustrated in Figure 55 are observed:

(a) Maximum tensile longitudinal stress is reduced by 60%.

(b) Radial stresses are negligible,

(c) Circumferential and shear stresses are considerably reduced and

(d) Compressive stresses at free end are magnified considerably.

Of particular interest is the shifting of the points of maximum shear and longitudinal stresses towards the free end. Perry and Thompson [16] have indicated that the point of maximum bond stress precedes the propagation of the rupture point (page 32). The present analysis confirms this observation. The reduction of the circumferential stresses is in direct contrast to the results obtained by Lutz (page 86). However, Lutz simulated slip of deformed bars in which the ribs produce large splitting stresses. The experimental investigation has shown that splitting stresses are not large enough in the case of plain bars to cause bursting. This fact is substantiated by the present analysis.

5.4) CONCLUSIONS.

(a) 'Perfect Bond' Analysis.

The 'perfect bond' analysis established that the modified test method produces slip results which are more representative of those found in actual structural members, than does the conventional test. Displacement of the concrete at the loaded end, was shown in the experimental investigation (page 65)to affect the measurement of slip at the concrete surface and this is confirmed by the finite element analysis. In this respect, the measurement of loaded end slip in the conventional test may be in error up to 30% at low loads. The large tensile longitudinal stresses shown to be developed by both test methods clearly suggest that transverse cracks would be produced. The affects of the cracks on the measurement of loaded end slip is inhibited by the conventional test method. However, displacement of the loaded end concrete surface due

to cracks within the concrete matrix is taken into account by the modified test. Further, it was found that considerable differences in stress magnitude and distribution are manifest by the two types of test. Large compressive longitudinal stresses are indicated at the loaded end of the conventional test which are not manifest in the modified test and differences in magnitude of radial and circumferential stresses are also found. These differences would be magnified by using a shorter specimen length.*

(b) Analysis with Assumed Slip and Separation.

Slip and separation of concrete from the reinforcing steel caused the stresses to be more evenly distributed than in the perfect bond analysis. In particular, the results indicated that:

(i) Large reductions in all stresses are manifest.

(ii) The point of maximum bond shear stress moves towards the free end with increased slip.

(iii) The linkage element provides a simple method of simulating slip of plain reinforcing bars in concrete.

The writer suggests that a case has been made for the validity of the findings from the modified pullout technique developed for this investigation.

*The dimensions of the specimens in the present investigation were bound by the primary consideration of determining the effect of temperature on bond.

REFERENCES.

1) Peattie, K.R. and Pope, J.A., 'Effect of age on concrete on bond resistance'. A.C.I.* Journal, V. 52, Feb. 1956, pp 661-672.

2) Lutz, L.A. and Gergely, P., 'Mechanics of bond and slip of deformed bars in concrete. A.C.I. Journal, V.64, Nov. 1967, pp 711-720.

3) Brown, C.B., 'Bond failure between steel and concrete'. Journal of the Franklin Institute, V. 282, No. 5, Nov. 1966, pp 271-290.

4) Rehm, G., 'The fundamental law of bond'. Symposium on Bond and Crack Formation in Reinforced Concrete, Proceedings (Stockholm, 1957) Rilem, Paris.

5) Rehm, G., 'Stress distribution in reinforcing bars embedded in concrete'. Symposium on Bond and Cracking Formation in Reinforced Concrete, Proceedings, (Stockholm, 1957) Rilem, Paris.

6) Watstein, D., 'Distribution of bond stress in concrete pullout specimens'. A.C.I. Journal, V. 18, No. 9, May 1947, pp 1041-1052.

7) Clark, R.P., 'Comparative bond efficiency of deformed concrete reinforcing bars'. A.C.I. Journal, V.18., No. 4, Dec. 1946, pp 381-399.

8) Ferguson, P.M., Breen, J.E. and Thompson, I.N. 'Pull-out tests on high strength reinforcing bars'. A.C.I. Journal, V. 61, Aug. 1965, pp 933-948.

9) Rostacy, F.S. and Hognestad, E., 'Pilot bond tests on large reinforcing bars'. A.C.I. Journal, Nov. 1970, pp 576-579.

10) Abrahms, D. 'Tests of bond between concrete and steel'. Bulleting No. 71, University of Illinois, Dec. 1913.

*American Concrete Institute.

11) Kemp, F.S., Brezny, F.S. and Unterspan, J.C., 'Effect of rust and scale on the bond characteristics of deformed reinforcing bars'. A.C.I. Journal, V. 65, Sept. 1968, pp 743-755.

12) Johnston, B. and Cox, C., 'The strength of rusted deformed bars'. A.C.I. Journal, V. 37, 1941.

13) Lutz, L.A. 'Information on the bond of deformed bars from special pullout tests'. A.C.I. Journal, Nov. 1970, pp 885-887.

14) Clark, A.P., 'Bond of concrete reinforcing bars'. A.C.I. Journal, V. 21, No. 3, Nov. 1949, pp 161-183.

15) Bernander, K.G., 'An investigation of bond by means of strain measurements in high tensile bars embedded in long cylindrical pullout specimens'. Symposium on Bond and Crack Formation in Reinforced Concrete, Proccedings. (Stockholm, 1957,) Rilem, Paris.

16) Perry, E.S. and Thompson, J.N., 'Bond stress distribution on reinforcing steel in beam and pullout specimens. A.C.I. Journal, V. 66, Aug. 1966, pp 865-874.

17) Plowman, J.M., 'Maturity and strength of concrete'. Magazine of Concrete Research, V. 8, No. 22, Mar. 1956, pp 13-22.

18) Zienkiewitz, O.C., and Holister, G.S., 'Stress analysis - Recent developements in numerical and experimental methods.' John Wiley and Sons, New York,1965.

19) Plowman, J.M., 'The relation between strength and maturity for ordinary Portland cement concrete'. Magazine of Concrete Research. Aug. 1957.

20) Harada, T., Takeda, J., Yamane, S., and Eurumura, F., 'Strength, elasticity and thermal properties of concrete subjected to elevated temperatures. American Concrete Institute Seminar on Concrete for Nuclear Reactors. West Berlin, Oct. 1970.

21) Mathey, R.G., and Watstein, D. 'Investigation of bond in beam and pullout specimens with high-yield-strength deformed bars'. A.C.I. Journal, V. 571, Mar. 1961, pp 1071.

22) A.S.T.M. (234-571), 'Comparing concretes on the basis of bond developed with reinforcing steel.'

23) Plowman, J.M. 'The measurement of bond strength'. Symposium on Bond And Crack Formation in Reinforced Concrete, Proceedings (Stockholm, 1957) Rilem, Paris.

24) Untrauer, R.E. and Henry, 'Influence of normal pressure on bond strength'. A.C.I. Journal, V. 62, No. 5, May 1965, pp 577-586.

25) Brown, C.B. and Syabo S.Z., 'A study of bond between steel and restrained Expanding Concrete'. Magazine of Concrete Research, V. 20, No. 62, Mar. 1968.

26) Taylor, B.A. and Broms, B.B. 'Shear bond strength between coarse aggregate and cement paste on mortar'. A.C.I. Journal, V. 61, No. 8, Aug. 1964, pp 939-958.

27) Saimann, J.C. and Washa, G.W., 'Variation of mortar and concrete properties with temperature'. A.C.I. Journal, V. 54, No. 5, 1957, pp 303-325.

28) Lankard, D.R. ,Birkeimer, D.L., Fondrieste, F.F., and Snyder, M.J., 'The effects of moisture content on the structural properties of Portland Cement concrete exposed to temperatures up to 500°C'. Research Report, Battelle Memorial Institute, Ohio State University, Columbus, Ohio.

29) Hsu, T.C., and Slate, F.O., 'Tensile bond strength between coarse aggregate and cement paste or mortar'. A.C.I. Journal, V. 60, Ap 1963, p 465.

30) Campbell-Allen, D. and Desai, P.M., 'The influence of aggregate on the behaviour of concrete at elevated temperature'. Nuclear Engineering and

Design. N. 6, 1967.

31) Campbell-Allen, D., Low, E.W.W., and Roper, H., 'An investigation on the effects of elevated temperatures on concrete for nuclear reactor vessels'. Nuclear Structural Engineering, V.,2, 1965, pp 382-388.

32) Zoldners, N.G., 'Effect of high temperatures on concretes incorporating different aggregates'. Canadian Mines Branch Research Report. R 14.

33) Goodier, J.N., 'An extension of Saint Venants Principle, with applications. Journal of Applied Physics., V. 13, No. 3, 1942, pp 167-171.

34) Broms, B.B., 'Stress distribution in reinforced concrete members with tension cracks'. A.C.I. Journal, V. 62, No. 9, Sept. 1965, pp 1095-1108.

35) Ngo, D. and Scordelis, A.C. 'Finite element analysis of reinforced concrete beams'. A.C.I. Journal, V. 65, Mar. 1967, pp 152-163.

36) Lutz, L.A.A. 'Analysis of stresses in concrete near a reinforcing bar due to bond and transverse cracking'. A.C.I. Journal, Oct. 1970, pp 778-787.

37) U.S. Bureau of Reclamation, Concrete Manual, 4th Edition, Denver, Colorado, Oct. 1942, pp26.

38) Fulton F.S. Concrete Technology. Portland Cement Institute, Johannesburg. Fourth Edition,1969.

39) Smithells, C.J., 'Metals Reference Book'. 3rd Edition, V. 2, London, Butterworths.